Semiconductor Quantum Dots and Quantum Dot Arrays and Applications of Multiple Exciton Generation to Third-Generation Photovoltaic Solar Cells

A. J. Nozik,*[,†,‡] M. C. Beard,[†] J. M. Luther,[†] M. Law,[§] R. J. Ellingson,[||] and J. C. Johnson[†]

The National Renewable Energy Laboratory, 1617 Cole Boulevard, Golden, Colorado 80401, United States, Department of Chemistry and Biochemistry, University of Colorado, Boulder, Colorado 80309, United States, Department of Chemistry, University of California, Irvine, Irvine, California 92697, United States, and Department of Physics and Astronomy, University of Toledo, Toledo, Ohio 43606, United States

Received August 25, 2009

Contents

1. Introduction

Semiconductors show dramatic quantization effects when charge carriers (electrons and holes) are confined by potential barriers to small regions of space where the dimensions of the confinement are less than the de Broglie wavelength of the charge carriers, or equivalently, the nanocrystal diameter is less than twice the Bohr radius of excitons in the bulk material. The length scale at which these effects begin to occur in semiconductors is less than about 25 to 10 nm depending upon effective masses. When the charge carriers are confined by potential barriers in three spatial dimensions, this regime is termed a quantum dot (QD). Two-dimensional confinement produces quantum wires or rods, while one-dimensional confinement produces quantum films. QDs can be formed either by epitaxial growth from the vapor phase (molecular beam epitaxy (MBE) or metallo-organic chemical vapor deposition (MOCVD) processes) or via chemical synthesis (colloidal chemistry or electrochemistry). QDs are also frequently referred to as nanocrystals (NCs). However, the term nanocrystal covers a range of shapes other than spherical in the nanoscale, such as nanowires, nanorods, nanotubes and nanoribbons,[1−7] nanorings,[8−11] and nanotetrapods.[12−14] The nanocrystals referred to here are semiconductor particles quantum confined in three dimensions.

The use of semiconductor nanocrystals that exhibit quantization effects in solar photoconversion devices (mainly quantum dots, quantum wires, and quantum rods) is presently attracting a great level of interest.[15−23] Such QD-based devices used as photovoltaic cells are now labeled third-generation or next-generation PV[24,25] because new advances in the photophysics allows for the possibility of these inexpensive materials to be incorporated into device structures with potential efficiency much higher than the thermodynamic limit for single junction bulk solar cells. The concept of the use of quantization effects in semiconductors to enhance solar photoconversion performance that now forms the basis for much of what is now known as third-generation solar conversion originated in the late 1970s and early 1980s, with the concept of hot electron utilization and its enhancement through quantum confinement in various semiconductor nanostructures.[26−30]

Beginning in the early 1980s, quantum dots of groups II−VI, III−V, IV−VI, and IV were specifically synthesized to investigate size quantization effects; prior to this period, nanocrystals had been utilized in various materials to achieve certain effects through empirical exploration such as color control in stained glass, but their quantized nature was not recognized until the 1970s. This early work has been reviewed by several authors.[31−40] CdS, CdSe, CdTe, InP, GaAs, GaP, GaN, GaInP, core−shell InP/$ZnCdSe_2$, Ge, and Si QDs were among the early reported syntheses.[31−38]

Beginning in the 1990s and extending to today, the syntheses of NCs and QDs have improved greatly; these advances include lower reaction temperatures, one-pot syntheses, better size control and size dispersion, new materials systems, better shape control, heterostructured particles such as core−shell QDs or end-on attachment, and better control and understanding of surface chemistry. These

* To whom correspondence should be addressed. E-mail: anozik@nrel.gov.
[†] The National Renewable Energy Laboratory.
[‡] University of Colorado.
[§] University of California, Irvine.
[||] University of Toledo.

10.1021/cr900289f
Published on Web 10/14/2010

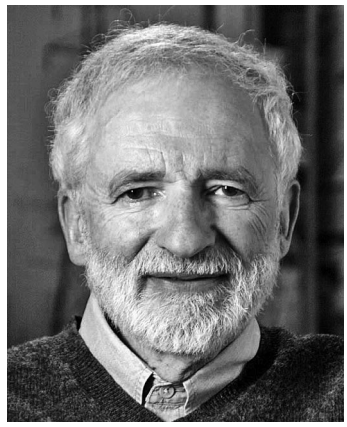

Dr. Arthur J. Nozik is a Senior Research Fellow at the U.S. DOE National Renewable Energy Laboratory (NREL), Professor Adjoint in the Department of Chemistry and Biochemistry at the University of Colorado, Boulder, and a Fellow of the NREL/University of Colorado Renewable and Sustainable Energy Institute. In 2009, Nozik was selected as Associate Director of a joint Los Alamos National Lab/NREL Energy Frontier Research Center for DOE called Center for Advanced Solar Photophysics. Between 2006 and 2009 he served as the Scientific Director of the Center for Revolutionary Solar Photoconversion under the Colorado Renewable Energy Collaboratory. Nozik received his BChE from Cornell University in 1959 and his Ph.D. in Physical Chemistry from Yale University in 1967. Before joining NREL in 1978, then known as the Solar Energy Research Institute (SERI), he conducted research at the Materials Research Center of the Allied Chemical Corporation (now Honeywell, Inc.). Dr. Nozik's research interests include size quantization effects in semiconductor quantum dots and quantum wells, including multiple exciton generation from a single photon; the applications of unique effects in nanostructures to advanced approaches for solar photon conversion; photogenerated carrier relaxation dynamics in various semiconductor structures; photoelectrochemistry of semiconductor−molecule interfaces; photoelectrochemical energy conversion; photocatalysis; optical, magnetic, and electrical properties of solids; and Mössbauer spectroscopy. He has published over 250 papers and book chapters in these fields, written or edited five books, holds 11 U.S. patents, and has delivered over 275 invited talks at universities, conferences, and symposia. He has served on numerous scientific review and advisory panels, chaired and organized many international and national conferences, workshops, and symposia, and received several awards in solar energy research, including the 2009 Science and Technology Award from the Intergovernmental Renewable Energy Organization associated with the United Nations, the 2008 Eni Award from the President of Italy, and the 2002 Research Award of the Electrochemical Society. Dr. Nozik has been a Senior Editor of The *Journal of Physical Chemistry* from 1993 to 2005 and is on the editorial advisory board of the *Journal of Energy and Environmental Sciences* and the *Journal of Solar Energy Materials and Solar Cells*. A Special Festschrift Issue of the *Journal of Physical Chemistry* honoring Dr. Nozik's scientific career appeared in the December 21, 2006 issue. Dr. Nozik is a Fellow of the American Physical Society and a Fellow of the American Association for the Advancement of Science; he is also a member of the American Chemical Society, the Electrochemical Society, and the Materials Research Society.

Matthew C. Beard is a Senior Scientist at the National Renewable Energy Laboratory. He received his B.Sc. And M.Sc. Degrees in Chemistry from Brigham Young University in 1997 and Ph.D. Degree in Physical Chemistry from Yale University in 2002. He spent a year at the National Institute of Science and Technology as a National Research Council postdoctoral fellow before joining NREL, working with Arthur J. Nozik. Matt is currently investigating quantum dots and nanostructures for high efficiency solar energy conversion.

Joseph M. Luther obtained B.Sc. Degrees in Electrical and Computer Engineering from North Carolina State University in 2001. His interest in photovoltaics sent him to the National Renewable Energy Laboratory (NREL) to pursue graduate work. He obtained a Masters of Science in Electrical Engineering from the University of Colorado and a Ph.D. in Physics from Colorado School of Mines while working in NREL's Basic Sciences division. As a postdoctoral fellow, he studied under Paul Alivisatos at the University of California and Lawrence Berkeley National Laboratory. In 2009, he rejoined NREL as a senior research scientist. His research interests lie in the growth, electrical coupling, and optical properties of colloidal nanocrystals and quantum dots.

advances have been described in several recent reviews and papers[31,41−54] and will not be reviewed here. Reviews of work on nanowires, rods, rings, tubes, ribbons, and tetrapods are available.[1−10,12−14,55]

Here, we will first briefly summarize the general principles of QD synthesis using our previous work on InP as an example. Then we will focus on QDs of the IV−VI Pb chalcogenides (PbSe, PbS, and PbTe) and Si QDs because these were among the first QDs that were reported to produce multiple excitons upon absorbing single photons of appropriate energy (a process we call multiple exciton generation (MEG)). We note that in addition to Si and the Pb−VI QDs, two other semiconductor systems (III−V InP QDs[56] and II−VI core−shell CdTe/CdSe QDs[57]) were very recently reported to also produce MEG. Then we will discuss photogenerated carrier dynamics in QDs, including the issues and controversies related to the cooling of hot carriers and the magnitude and significance of MEG in QDs. Finally, we will discuss applications of QDs and QD arrays in novel quantum dot PV cells, where multiple exciton generation from single photons could yield significantly higher PV conversion efficiencies.

2. Synthesis of Colloidal Quantum Dots

2.1. Solution Synthesis

The most common approach to the synthesis of colloidal ionic QDs is the controlled nucleation and growth of particles in a solution of chemical precursors containing the metal and the anion sources (controlled arrested precipitation).[48,58−60] The technique of forming monodispersed colloids is very old and can be traced back to the synthesis of gold colloids

Justin Johnson received a B.A. in Chemistry and Physics from Macalester College in 1999 and a Ph.D. Degree in Chemistry from the University of California at Berkeley in 2004 under the supervision of Prof. Richard Saykally, investigating lasing and charge relaxation dynamics in single semiconductor nanostructures using nonlinear optical spectroscopy and near-field microscopy. In 2004, he began as a postdoctoral researcher jointly with Dr. Arthur Nozik at the National Renewable Energy Laboratory (NREL) and Prof. Josef Michl of the University of Colorado at Boulder, investigating ultrafast photophysical processes in semiconductor quantum dots and singlet fission in molecular systems. He became a staff scientist at NREL in 2008 and is currently a Senior Scientist in the Chemical and Materials Science Center, focusing primarily on the understanding of exciton multiplication phenomena in organic and inorganic light absorbers using ultrafast spectroscopy.

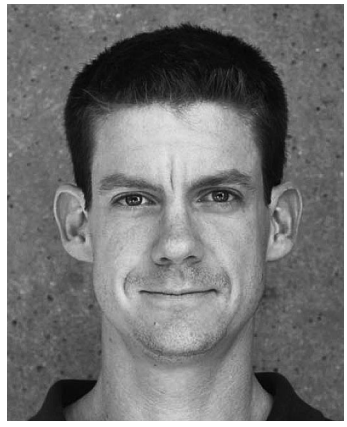

Professor Matt Law joined the Chemistry Department at the University of California, Irvine in 2008. He received his Ph.D. in Chemistry from the University of California, Berkeley in 2006, where he investigated the synthesis, properties, and device applications of oxide nanowires under the direction of Professor Peidong Yang. For this work, he was named a 2005 Young Investigator by the Division of Inorganic Chemistry of the American Chemical Society and was awarded the 2006 IUPAC Prize for Young Chemists. His postdoctoral research with Professor Arthur Nozik at the National Renewable Energy Laboratory focused on the development of quantum dot solar cells and photoelectrochemical water-splitting devices. Professor Law's research interests are driven by the challenges of energy conversion and storage, chemical sensing, pollution remediation, and the conservation of biodiversity. He has published 30 papers (cited over 5000 times) and five patents. His group at UC Irvine synthesizes and studies nanostructured materials and devices for solar energy utilization."

by Michael Faraday in 1857. A common method for II−VI and IV−VI colloidal QD formation is to rapidly inject a solution of chemical reagents containing the group II, IV, and VI species into a hot and vigorously stirred solvent containing molecules that can coordinate with the surface of the precipitated QD particles.[48,58,60−63] Consequently, a large number of nucleation centers are initially formed, and the coordinating ligands in the hot solvent prevent or limit particle growth via Ostwald ripening. Although often not

Randy Ellingson is an Associate Professor in the Department of Physics and Astronomy at the University of Toledo, a faculty member of the Wright Center for Photovoltaics Innovation and Commercialization, and a Senior Research Associate at the National Renewable Energy Laboratory. His research focuses on (a) understanding the fundamental properties of colloidal semiconductor nanocrystals and nanocrystalbased thin film assemblies for photovoltaics and (b) applying ultrafast laser spectroscopy to study the dynamics of photogenerated charge carriers in nanocrystalline and molecular-scale materials, as well as thin film absorbers. Long term goals include developing inexpensive processes whereby low-toxicity and Earth-abundant materials can be used to fabricate very efficient photovoltaic devices. He received his B.A. in Physics from Carleton College in 1987, and received the M.Sc. and Ph.D. Degrees in Applied Physics in 1990 and 1994 from Cornell University. Following 14 years as a research scientist at the National Renewable Energy Laboratory, Randy joined the University of Toledo in 2008. He served as a Detailee to the U.S. DOE's Office of Basic Energy Sciences in 2005 and provided technical and organizational assistance with the Workshop on *Basic Research Needs for Solar Energy Utilization*. He served as Co-Chair for the Symposium on Light Management in Photovoltaic Devices—Theory and Practice, at the 2008 Materials and Research Society Spring Meeting.

necessary now with well developed materials, further improvement of the resulting size distribution of the QD particles can be achieved through size selective precipitation,[60,61] whereby slow addition of a nonsolvent and subsequent centrifugation of the colloidal solution of particles causes precipitation of the larger-sized particles (the solubility of molecules with the same type of chemical structure decreases with increasing size). This process can be repeated several times to narrow the size distribution of II−VI colloidal QDs to several percent of the mean diameter.[60,61]

As an example of an early III−V QD synthesis, an indium salt (for example, $In(C_2O_4)Cl$, InF_3, or $InCl_3$) was reacted with trimethylsilylphosphine $\{P[Si(CH_3)_3]_3\}$ in a solution of trioctylphosphine oxide (TOPO) and trioctylphosphine(TOP) to form a soluble InP organometallic precursor species that contains In and P in a 1:1 ratio.[64,65] The precursor solution was then heated at 250−290 °C for 1−6 days, depending upon desired QD properties. Use of TOPO/TOP as a colloidal stabilizer was first reported by Murray, Norris, and Bawendi,[61] who showed the remarkable ability of phosphonate complexes to stabilize semiconductor CdSe QDs at high temperature. Different particle sizes of InP QDs were obtained by changing the temperature at which the solution was heated. The duration of heating only slightly affected the particle size but did improve the QD crystallinity. The precursor had a high decomposition temperature (>200 °C); this is advantageous for the formation of InP quantum dots because the rate of QD formation is controlled by the rate of decomposition of the precursor. After heating, the clear reaction mixture contained InP QDs, byproducts of the synthesis, products resulting from TOPO/TOP thermal

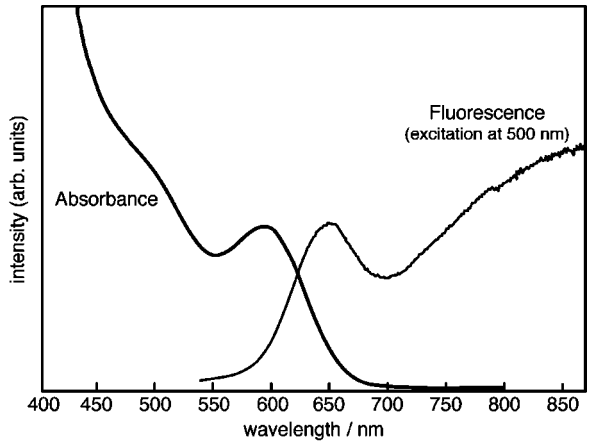

Figure 1. Absorption and emission spectra at 298 K of untreated 32 Å InP QDs. Reprinted with permission from ref 66. Copyright 1996 American Institute of Physics.

decomposition, and untreated TOP and TOPO. Anhydrous methanol was then added to the reaction mixture to flocculate the InP nanocrystals. The flocculate was separated and completely redispersed in a mixture of 9:1 hexane and 1-butanol containing 1% TOPO to produce an optically clear (nonscattering) colloidal solution. The process of dispersion in the mixture of hexane and 1-butanol and flocculation with anhydrous methanol was repeated several times to purify and isolate a pure powder of InP nanocrystals that was capped with TOPO. Repetitive selective flocculation by methanol gradually stripped away the TOPO capping group; thus, TOPO (1%) was always included in the solvent when the QDs were redissolved in order to maintain the TOPO cap on the QDs. Fractionation of the QD particles into different sizes was obtained by selective precipitation methods;[61] this technique reduced the size distribution of the initial colloid preparation to about 10%.

The resulting InP QDs contained a capping layer of TOPO, which could be readily exchanged for several other types of capping agents such as thiols, furan, pyridines, amines, fatty acids, sulfonic acids, and polymers. Finally, they could be studied in the form of colloidal solutions, powders, or dispersed in transparent polymers or organic glasses (for low temperature studies); capped InP QDs recovered as powders can also be redissolved to form transparent colloidal solutions.

Recent improved processes for formation of InP QDs have been reported.[42,50] These improvements include lower reaction temperature (160 °C), narrower size distribution, better ligand stabilization chemistry, and synthesis via "green" chemistry.

The room temperature absorption and uncorrected emission spectra of InP QDs with a mean diameter of 32 Å prepared by the initial methods[64,65] are shown in Figure 1. The absorption spectrum shows a broad excitonic peak at about 590 nm and a shoulder at 490 nm; the substantial inhomogeneous line broadening of these excitonic transitions arises from the QD size distribution. The transitions are excitonic because the QD radius is less than the exciton Bohr radius. The photoluminescence (PL) spectrum (excitation at 500 nm) shows two emission bands: a weaker one near the band edge with a peak at 655 nm and a second, stronger, broader band that peaks above 850 nm. The PL band with deep red-shifted subgap emission peaking above 850 nm is attributed to radiative surface states on the QDs produced by phosphorus vacancies.[66,67]

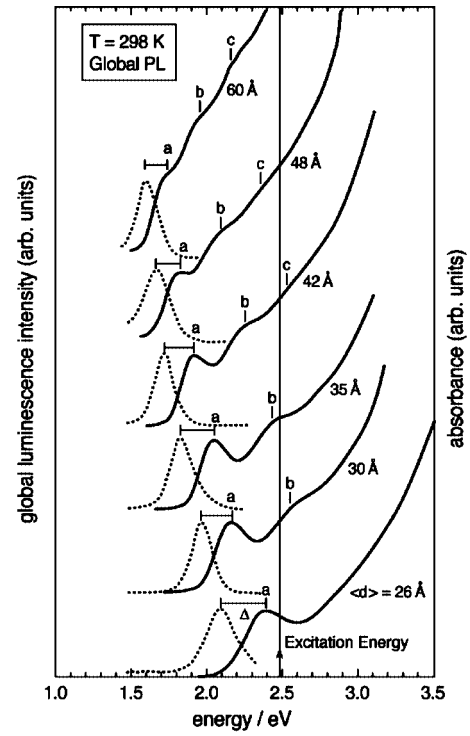

Figure 2. Absorption and emission spectra of HF-treated InP QDs for different mean diameters. a, b, and c mark the excitonic transitions apparent in the absorption spectra. All samples were excited at 2.5 eV. Reprinted with permission from ref 68. Copyright 1997 American Chemical Society.

The room temperature absorption spectra as a function of QD size ranging from 26 to 60 Å (measured by TEM) are shown in Figure 2; the red-shifted deep trap emission from the as-prepared colloidal QDs was eliminated by etching the QDs in HF. The absorption spectra show one or more broad excitonic peaks; as expected, the spectra shift to higher energy as the QD size decreases.[68] The color of the InP QD samples changes from deep-red (1.7 eV) to green (2.4 eV) as the diameter decreases from 60 to 26 Å. Bulk InP is black, with a room temperature band gap of 1.35 eV and an absorption onset at 918 nm. Higher energy transitions above the first excitonic peak in the absorption spectra can also be easily seen in QD samples with mean diameters equal to or greater than 30 Å. The spread in QD diameters was generally about 10%. Figure 2 also shows typical room temperature global emission spectra of the InP colloids as a function of QD diameters. We define global PL as that observed when the excitation energy is much higher than the energy of the absorption threshold exhibited in the absorption spectrum produced by the ensemble of QDs in the sample. That is, the excitation wavelength is well to the blue of the first absorption peak for the QD ensemble, and therefore a large fraction of all the QDs in the sample are excited. The particle diameters that are excited range from the largest in the ensemble to the smallest, which has a diameter that produces a blue-shifted band gap equal to the energy of the exciting photons. In Figure 2, the excitation energy for all QD sample ensembles was 2.48 eV, well above their absorption onset in each case. The global PL emission peaks ("non-resonant") in Figure 3 are very broad (line width of 175−225 meV) and are red-shifted by 100−300 meV as the QD size decreases from 60 Å to 26 Å.[68] The broad PL line width is caused by the inhomogeneous line broadening arising from the ∼10% size distribution. The large global red-shift and

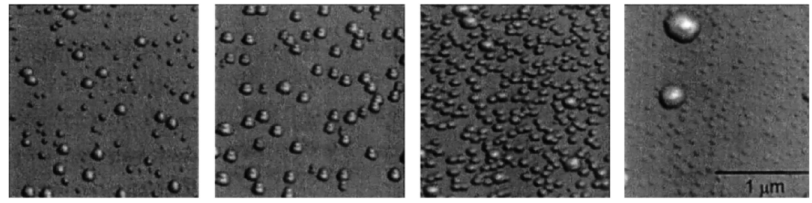

Figure 3. Evolution of Stranski−Krastinow InP islands grown on (100) AlGaAs at 620 °C by MOCVD for increasing amounts of deposited InP [expressed as monolayers (ML)]. The scale of each scan is 2 μm × 2 μm.

its increase with decreasing QD size is attributed to the volume dominance of the larger particles in the size distribution; the larger QDs will absorb a disproportionally larger fraction of the incident photons relative to their number fraction and will show large red-shifts (because the PL excitation energy is well above their lowest transition energy) that will magnify the overall red-shift of the QD ensemble.

2.2. III−V Quantum Dots Grown via Vapor Phase Deposition

Semiconductor quantum dots can also be formed via deposition from the vapor phase onto appropriate substrates in MBE or MOCVD reactors. There are two modes of formation. In one, termed Stranski−Krastinow (S−K) growth, nanometer-sized islands can form when several monolayers (about 3−10) of one semiconductor are deposited upon another and there is large lattice-mismatch (several %) between the two semiconductor materials; this has been demonstrated for Ge/Si, InGaAs/GaAs, InP/GaInP, and InP/AlGaAs. For these highly strained systems, epitaxial growth initiates in a layer-by-layer fashion and transforms to 3D island growth above four monolayers to minimize the strain energy contained in the film (see Figure 3). The islands then grow coherently on the substrate without generation of misfit dislocations until a certain critical strain energy density, corresponding to a critical size, is exceeded. Beyond the critical size, the strain of the film/substrate system is partially relieved by the formation of dislocations near the edges of the islands. Coherent SK islands can be overgrown with a passivating and carrier-confining epitaxial layer to produce QDs with good luminescence efficiency. The optical quality of such overgrown QD samples depends upon the growth conditions of the capping layer.

The second approach is to first produce a near surface quantum well (formed from 2-D quantum films) and then deposit coherent S−K islands on top of the outer barrier layer of the QW that have a large lattice mismatch with the barrier that produces a compressive strain in the island. The large resultant strain field can extend down into the QW structure by about one island diameter, thus penetrating through the outer barrier and well regions. This strain field will dilate the lattice of the QW and lower the band gap beneath the S−K islands to produce a quantum dot with 3-dimensional confinement. One unique aspect of this QD is that the well and barrier regions are made of the same semiconductor. The S−K islands are referred to as stressor islands; such types of stress-induced InGaAs and GaAs QDs have been reported for InP stressor islands on a GaAs/InGaAs/GaAs QW and for InP stressor islands on an AlGaAs/GaAs/AlGaAs QW.

Much research has been done on QDs grown by epitaxial approaches through the gas phase, and several reviews are available.[69,70] A very recent paper demonstrates very low broadening of absorption spectra in InGaAs/GaAs QDs via MOCVD with very large s−p separations.[71]

3. Relaxation Dynamics of Photogenerated Carriers In QDs

When the energy of a photon absorbed in semiconductor QDs is greater than the lowest energy excitonic transition (frequently termed the QD band gap although no energy bands exist in isolated QDs), photogenerated electrons and holes (usually in the form of excitons) are created with excess energy above the lowest exciton energy; these energetic electron−hole pairs are termed hot carriers (or hot excitons if the e^- and h^+ are coupled by confining the carriers to small volumes as in QDs). The fate of this excess energy can follow several paths: (1) it can be dissipated as heat through electron−phonon interactions or Auger processes as the carriers relax to their lowest state, (2) a second electron−hole pair can be created by a process similar to the inverse of Auger recombination if the *excess* energy is at least equivalent to the QD band gap, and (3) the electrons and holes can separate and the excess energy can be converted to increased electrical free energy via a photovoltaic effect or stored as additional chemical free energy by driving more endoergic electrochemical reactions at the surface.[72] The efficiency of photon conversion devices, such as photovoltaic and photoelectrochemical cells, can be greatly increased if paths (2) or (3) can dominate over path (1). Path (1) is generally a fast process in bulk semiconductors that occurs in a few ps or less if the photogenerated carrier density is less than about 5×10^{17} cm^{-3}.[73−75] The hot electron relaxation, or cooling time, in bulk semiconductors can be increased by 2 orders of magnitude when the photogenerated carrier density is increased above about 5×10^{18} cm^{-3} by a process termed "hot phonon bottleneck".[73,75,76] QDs are intriguing because it has been predicted that slow cooling of energetic electrons can occur in QDs at low photogenerated carrier densities,[26,28,30,77−79] specifically at light intensities corresponding to the solar insolation on earth. However, this effect (simply called "phonon bottleneck") is controversial because several relaxation channels could in principle bypass the predicted slow electron−phonon cooling process. Many experimental results show large variations in cooling dynamics, some supporting a phonon bottleneck and others contradicting a phonon bottleneck (see discussion below in III-A).

The first prediction of slowed cooling at low light intensities in quantized structures was made by Boudreaux, Williams, and Nozik.[28] They anticipated that cooling of carriers would require multiphonon processes when the quantized levels are separated in energy by more than the fundamental phonon energy. They analyzed the expected slowed cooling time for hot holes at the surface of highly doped n-type TiO_2 semiconductors, where quantized energy

levels arise because of the narrow space charge layer (i.e., depletion layer) produced by the high doping level. The carrier confinement is this case is produced by the band bending at the surface; for a doping level of 1×10^{19} cm^{-3}, the potential well can be approximated as a triangular well extending 200 Å from the semiconductor bulk to the surface and with a depth of 1 eV at the surface barrier. The multiphonon relaxation time was estimated from

$$\tau_c \sim \omega^{-1} \exp(\Delta E/kT) \quad (1)$$

where τ_c is the hot carrier cooling time, ω is the phonon frequency, and ΔE is the energy separation between quantized levels. For strongly quantized electron levels, with $\Delta E > 0.2$ eV, τ_c could be >100 ps according to eq 1.

However, carriers in the space charge layer at the surface of a heavily doped semiconductor are only confined in one dimension, as in a quantum film. This quantization regime leads to discrete energy states which have dispersion in *k*-space. This means the hot carriers can cool by undergoing interstate transitions that require only one emitted phonon followed by a cascade of single phonon intrastate transitions; the bottom of each quantum state is reached by intrastate relaxation before an interstate transition occurs. Thus, the simultaneous and slow multiphonon relaxation pathway can be bypassed by single phonon events, and the cooling rate increases correspondingly.

More complete theoretical models for slowed cooling in QDs have been proposed by Bockelmann and co-workers[79,80] and Benisty and co-workers.[78,81] The proposed Benisty mechanism[78,81] for slowed hot carrier cooling and a phonon bottleneck in QDs requires that cooling only occurs via LO phonon emission. However, there are several other mechanisms by which hot electrons can cool in QDs. Most prominent among these is the Auger mechanism.[82] Here, the excess energy of the electron is transferred via an Auger process to the hole, which then cools rapidly because of its larger effective mass and smaller energy level spacing. Thus, an Auger mechanism for hot electron cooling can break the phonon bottleneck.[82] Other possible mechanisms for breaking the phonon bottleneck include electron−hole scattering,[83] deep level trapping,[84] and acoustical−optical phonon interactions.[85,86]

3.1. Experimental Determination of Relaxation/Cooling Dynamics and a Phonon Bottleneck in Quantum Dots

Over the past several years, many investigations have been published that explore hot electron cooling/relaxation dynamics in QDs and the issue of a phonon bottleneck in QDs; a review is presented in ref 72. As indicated above, the results are controversial, and it is quite remarkable that there are so many reports that both support[87−102] and contradict[89,103−114] the prediction of slowed hot electron cooling in QDs and the existence of a phonon bottleneck. A recent paper reports strong evidence for a phonon bottleneck in core−shell CdSe QDs,[87] but the energy regime is for states near the bottom of the spherical quantum well, not for high energy states.

One element of confusion that is specific to the discussion in this manuscript is that while some of these publications report relatively long hot electron relaxation times (tens of ps) compared to what is observed in bulk semiconductors, the results are reported as being not indicative of a phonon bottleneck because the relaxation times are not excessively long and PL is observed[115−117] (theory predicts infinite relaxation lifetime of excited carriers for the extreme, limiting condition of a phonon bottleneck; thus, the carrier lifetime would be determined by nonradiative processes and PL would be absent). However, because the interest here is on the relative rate of relaxation/cooling compared to the rate of electron transfer, slowed relaxation/cooling of carriers can be considered to occur in QDs if the relaxation/cooling times are greater than 10 ps (about an order of magnitude greater than that for bulk semiconductors). This is because previous work that measured the time of electron transfer from bulk III−V semiconductors to redox molecules (metallocenium cations) adsorbed on the surface found that electron transfer (ET) times can be sub-ps to several ps;[118−121] hence photoinduced hot ET can be competitive with electron cooling and relaxation if the latter is greater than tens of ps. Recent research reports evidence for hot ET in solar cells.[122]

4. Multiple Exciton Generation (MEG) in Quantum Dots

The discussion above demonstrates unique properties relating to management of hot electrons in highly confined systems. An additional and highly important process that is the focus of this review is a process called multiple exciton generation. The efficient formation of more than one photoinduced electron−hole (e^-−h^+) pair upon the absorption of a single photon is a process of current scientific interest and is potentially important for improving solar devices (photovoltaic and photoelectrochemical cells) that directly convert solar radiant energy into electricity or stored chemical potential in solar-derived fuels like hydrogen, alcohols, and hydrocarbons. Several papers describe the thermodynamics of this conversion process.[123,124] Conversion efficiency in photovoltaic devices can increase because the excess kinetic energy of electrons and holes produced by absorption of photons with energies above the bandgap can create additional e^-−h^+ pairs when the photon energy is at least twice the bandgap energy. The second requirement is that the extra electrons and holes must also be separated, transported, and collected to yield enhanced photocurrent. In present photoconversion cells, such excess kinetic energy is converted to heat and becomes unavailable for conversion to electrical or chemical free energy (see Figure 4), thus limiting the maximum thermodynamic conversion efficiency.

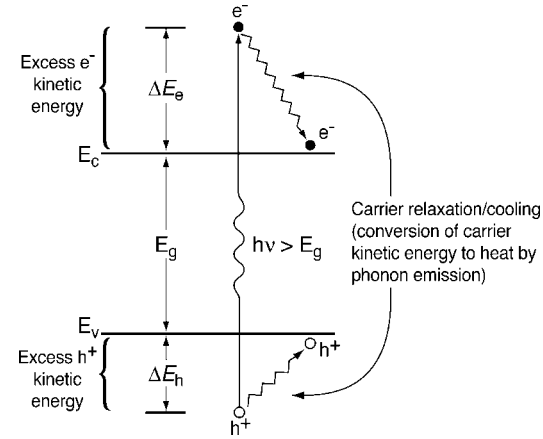

Figure 4. Hot carrier relaxation/cooling in semiconductors. Reprinted with permission from ref 68. Copyright 2001 Annual Reviews.

The creation of more than one e^-−h^+ pair per absorbed photon has been recognized for over 50 years in bulk semiconductors; it has been observed in the photocurrent of bulk p−n junctions in Si, Ge, PbS, PbSe, PbTe, and InSb[125−132] and in these systems is termed *impact ionization*. However, impact ionization (II) cannot contribute to improved quantum yields in present solar cells based on bulk Si, CdTe, $CuIn_xGa_{1-x}Se_2$, or III−V semiconductors because the maximum QY for II does not produce extra carriers until photon energies reach the ultraviolet region of the spectrum. In bulk semiconductors, the threshold photon energy for II exceeds that required for energy conservation alone because crystal momentum (**k**) must also be conserved. Additionally, the rate of II must compete with the rate of energy relaxation by phonon emission through electron−phonon scattering. It has been shown that the rate of II becomes competitive with phonon scattering rates only when the kinetic energy of the electron is many multiples of the bandgap energy (E_g).[133−135] In bulk semiconductors, the observed transition between inefficient and efficient II occurs slowly; for example, in Si, the II efficiency was found to be only 5% (i.e., total quantum yield = 105%) at $h\nu \approx 4$ eV ($3.6E_g$), and 25% at $h\nu \approx 4.8$ eV ($4.4E_g$).[129,136]

For Si, the overwhelmingly dominant material in photovoltaic cells today, impact ionization does not become significant until the incident photon energy exceeds 3.5 eV, an ultraviolet energy threshold above which less than 1% of the photons in the solar spectrum exist. Hence, impact ionization in bulk semiconductors is not a meaningful approach to increase the efficiency of conventional PV cells.

However, in quantum dots, the rate of Auger processes, including the inverse Auger process of MEG, can be greatly enhanced due to carrier confinement and the concomitantly increased e^-−h^+ Coulomb interaction;[137,138] the time scale for MEG has been reported to be <100 fs.[138] This ultrafast MEG rate is much faster than the hot exciton cooling rate produced by electron−phonon interactions, and MEG can therefore become efficient. Furthermore, crystal momentum is not a good quantum number for QDs and momentum need not be conserved; thus the threshold photon energy for the process to generate two electron−hole pairs per photon can approach values as low as twice the threshold energy for absorption (the absolute minimum to satisfy energy conservation). Lowering the threshold allows the solar spectrum to contribute more photons to the effect in materials with ideal bandgaps. The possibility of enhanced MEG in QDs was first proposed by Nozik,[21,72] and the original concept is shown in Figure 5.

In semiconductor QDs, the e^-−h^+ pairs become correlated because of the spatial confinement and thus exist as excitons rather than free carriers. Therefore, this is why we have labeled the formation of multiple excitons in quantum dots *multiple exciton generation* (MEG); free carriers can only form upon dissociation of the excitons.

Multiexcitons have been detected using several spectroscopic measurements which are consistent with each other. The first method is to monitor the signature of multiexciton generation using transient (pump−probe) absorption (TA) spectroscopy. The multiple exciton analysis relies only on data for delays >5 ps, by which time carrier multiplication and cooling are complete and the probe pulse is interrogating the exciton population at their lowest excited state (the band edges). In one type of TA experiment, the probe pulse monitors the interband bleach dynamics with excitation

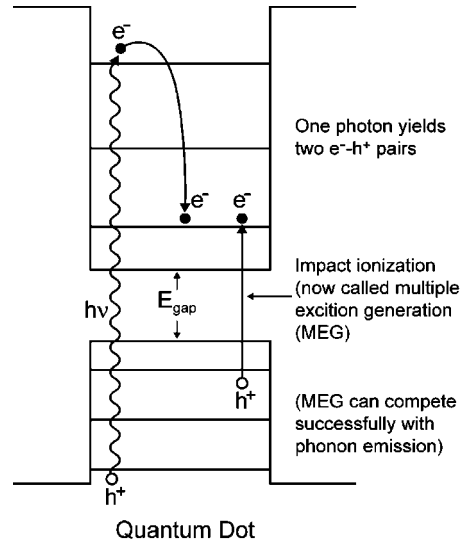

Figure 5. Multiple electron−hole pair (exciton) generation (MEG) in quantum dots. Reprinted with permission from ref 21. Copyright 2002 North Holland.

across the QD bandgap, whereas in a second type of experiment, the probe pulse is in the mid-IR and monitors the intraband transitions (e.g., $1S_e$−$1P_e$) of the newly created excitons (see Figure 6, left). In the former case, the peak magnitude of the initial early time photoinduced absorption change created by the pump pulse plus the faster Auger decay dynamics of the generated multiexcitons is related to the number of excitons created. In the latter case, the dynamics of the photoinduced mid-IR intraband absorption is monitored after the pump pulse (Figure 6, left). In refs 138 and 63, the transients are detected by probing either with a probe pulse exciting across the QD bandgap or with a mid-IR probe pulse that monitors the first $1S_e$−$1P_e$ intraband transition; both experiments yield the same MEG QYs.

The first report of exciton multiplication presented by Schaller and Klimov[139] for PbSe NCs reported an excitation energy threshold for the efficient formation of two excitons per photon at $3E_g$. But evidence has been reported that the threshold energy for MEG in PbSe QDs optical excitation is $2E_g$,[138] and it was shown that efficient MEG occurs also in PbS[138] (see Figure 6, right) and in PbTe nanocrystals.[63] Additional experiments observing MEG have been reported for PbSe,[140,141] CdSe,[142,143] PbTe,[63] InAs,[144,145] Si,[146] InP,[56] CdTe,[147] and CdSe/CdTe core−shell QDs.[57] For InP QDs, the MEG threshold was $2.1E_g$ and photocharging (see next paragraph for significance of QD charging for MEG) was shown not to be present in the QD samples.[57] For the CdSe/CdTe QDs, time-resolved photoluminescence (TRPL) was used to monitor the effects of multiexcitons on the PL decay dynamics.

However, some additional reports could not reproduce some of the reported positive MEG results[148−150] or, if MEG was indeed observed, the efficiency was much lower.[151] Thus, some controversy has arisen about the efficiency of MEG in QDs. The reason for this inconsistency has been attributed to the influence of QD surface treatments and surface chemistry on MEG dynamics compared to cooling dynamics[152] and in some cases to the effects of surface charge produced during transient pump−probe spectroscopic experiments to determine MEG quantum yields.[153] In the latter case, long-lived charge would produce trions after the absorption of an additional photon in the QDs in a pump−probe

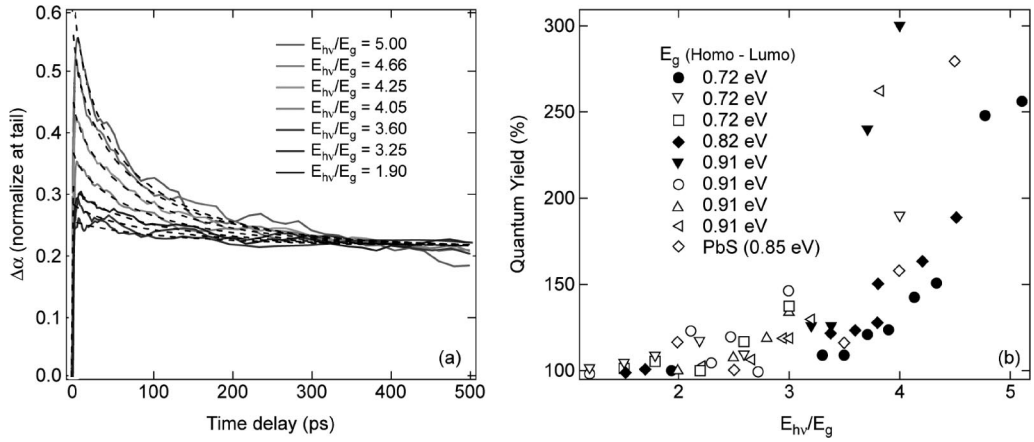

Figure 6. (left) Exciton population decay dynamics obtained by probing intraband (intraexciton) transitions in the mid-IR at 5.0 μm for a sample of 5.7 nm diameter PbSe QDs. (right) QY for exciton formation from a single photon vs photon energy expressed as the ratio of the photon energy to the QD bandgap (HOMO−LUMO energy) for three PbSe QD sizes and one PbS (diameter = 3.9, 4.7, 5.4, and 5.5 nm, respectively, and E_g = 0.91, 0.82, 0.73, and 0.85 eV, respectively). Solid symbols indicate data acquired using mid-infrared probe; open symbols indicate band edge probe energy. Quantum yield results are independent of the probe energy utilized. Reprinted with permission from ref 138 Copyright 2005 American Chemical Society.

experiment, which could interfere with the fast early time decay of transient absorption or bleaching signals that is the signature of MEG and lead to overestimation of the MEG QY.[153] However, recent work[56,140,154] shows that charging effects may not always be significant, and they are dependent upon the specific QD surface chemistry, photon fluence, photon energy, and QD size; in any case, the possibility of photocharging effects can be eliminated by flowing or stirring the colloidal suspension to refresh the sample volume of QDs being probed.[153,154] However, the possibility of charging needs to be considered for all experiments done on static solutions or solid state films and experiments done to ensure trion or trapped charge-influenced decay is not contributing to producing inaccurate values of the MEG efficiency.

4.1. MEG in Si QDs

As mentioned previously, Si is the prototypical material for solar cells and recent work has shown that colloidal QDs of Si produced via flowing silane gas through a high energy plasma[155,156] also demonstrate MEG with increased efficiency over bulk wafers or films. Silicon's indirect band structure yields extremely weak linear absorption at the bandgap, and thus one cannot readily probe a state-filling-induced bleach via this interband transition. Instead, the exciton population dynamics are probed by the method of photoinduced intraband absorption changes.

In ref 146, the first efficient MEG in Si NCs was reported using transient intraband absorption spectroscopy and the threshold photon energy for MEG was 2.4 ± 0.1E_g, and the quantum yield (QY) of excitons produced per absorbed photon reached 2.6 ± 0.2 at 3.4E_g. In contrast, for bulk Si the threshold for impact ionization is ~3.5E_g and the QY rises to only ~1.4 at 4.5E_g.[136] Highly efficient MEG in nanocrystalline Si at lower photon energies in the visible region (i.e., a threshold of 2E_g) has the potential to increase power conversion efficiency in Si-based PV cells toward a maximum thermodynamic limit of ~44% at standard AM1.5G solar intensity and with a staircase characteristic.

In the Si QD experiments,[146] the probe was mainly at 0.86 eV, well below the effective bandgap. However, it was verified that the photoinduced absorption dynamics did not depend on the probe energy over a broad range from 0.28 to ~1 eV. TA data below the threshold showed that the biexciton decay times for three different Si NC sizes depended linearly on the QD volume, in agreement with the Auger recombination (AR) mechanism. Thus, a new decay channel observed at high pump fluences was confirmed to be nonradiative AR.

When photoexciting above the energy conservation threshold for MEG (>2E_g) at low intensity so that each photoexcited NC absorbs on average less than one photon, multiexciton AR serves as a metric for MEG. Figure 7 shows the

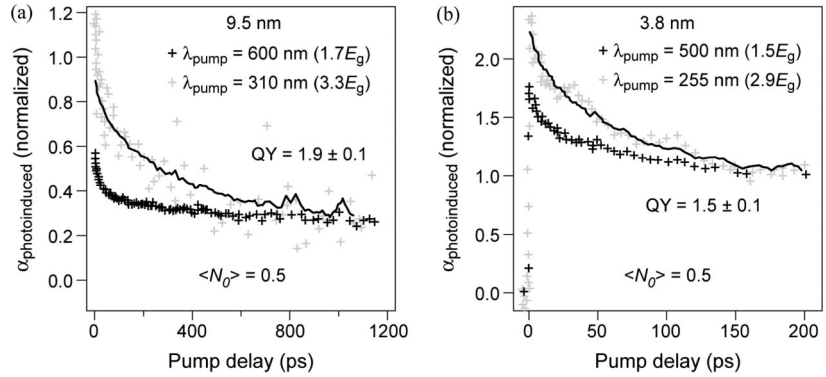

Figure 7. Photoinduced transient absorption (TA) dynamics for Si QDs. Left: TA photoexciting below and above the MEG threshold for 9.5 nm Si QDs. Right: TA photoexciting below and above the MEG threshold for 3.8 nm Si QDs. Reprinted with permission from ref 146. Copyright 2007 American Chemical Society.

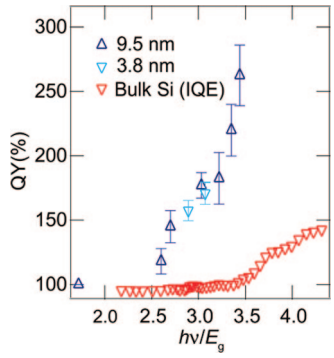

Figure 8. Compilation of all MEG QYs for the 9.5 (blue triangles) and 3.8 nm (light-blue triangles) Si QD samples. Red triangles are impact ionization quantum yields for bulk Si. Reprinted with permission from ref 146. Copyright 2007 American Chemical Society.

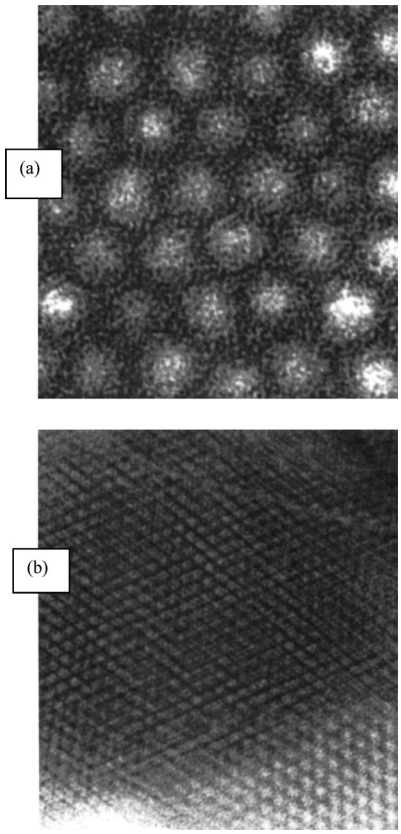

Figure 9. TEM of close-packed 3-D array of 57 Å InP QDs showing hexagonal order. The bottom panel is at a lower magnification and shows a monolayer step between the darker and lighter regions.

decay dynamics when $\langle N_0 \rangle$ is held constant at 0.5 at different pump wavelengths for the 9.5 and 3.8 nm samples, respectively. The black crosses are the decay dynamics for pump energies of 1.7 and $1.5E_g$ (below the MEG threshold), and the gray crosses are for photon energies of 3.3 and $2.9E_g$ (above the MEG threshold). The data at long times (>300 ps) in Figure 8 for the $3.3E_g$ pump are noisy, but the presence of the new fast decay component at times <300 ps is clearly evident. The data were modeled with only one adjustable parameter, the MEG efficiency, η.

By photoexciting above the energy conservation threshold for MEG ($>2E_g$) and at low intensity so that each photoexcited NC absorbs <1 one photon on average, the appearance in Figure 7 of fast multiexciton Auger recombination serves as a signature for MEG. The QYs for MEG in 9.5 and 3.8 nm diameter Si QDs are plotted vs photon energy normalized to the band gap ($h\upsilon/E_g$) in Figure 8 and compared to the results for bulk Si. Figure 9 shows that the onset of e−h pair multiplication occurs at lower photon energy and the QY rises more steeply after the onset of e−h pair multiplication compared to bulk Si. These features make Si QDs very appealing for application in solar photon conversion applications.

We note, however, that all the Si QD MEG determinations were conducted under static conditions (colloidal QDs were not stirred, flowed, nor spun). As discussed above, because there is a nonzero possibility that long-lived charge could be created during photoexcitation by the pump beam through fast trapping of an electron or hole at the QD surface and thus complicate or perhaps exaggerate the MEG QY through trion formation, the Si MEG experiments reported here need to be repeated using a flow or stirred system to ensure QD charging is not a confounding factor in determining MEG QYs. However, recent experiments[154] show that photocharging is nearly negligible in PbSe QDs at the low photon fluence used in the Si experiments and may thus be unlikely to affect the Si results.

5. Quantum Dot Arrays

A major area of semiconductor nanoscience is the formation of QD arrays and understanding the transport and optical properties of these arrays. One approach to form arrays of close-packed QDs is to slowly evaporate colloidal solutions of QDs: upon evaporation, the QD volume fraction increases and interaction between the QDs develops and leads to the formation of a self-organized QD film. Spin deposition and dip coating can also be used. Figure 9a shows the formation of a monolayer organized in a hexagonal network made with InP QDs 57 Å in diameter and which are capped with dodecanethiol; InP, QDs capped with oleylamine can form monolayers with shorter range hexagonal order. The QDs in these arrays have size distributions of about 10%, and with such a size distribution the arrays can only exhibit local order.

To form colloidal crystals with a high degree of order in the QD packing, the size distribution of the QD particles must have a mean deviation less than about 5% and uniform shape. Murray and co-workers[157] fabricated highly ordered 3-D superlattices of CdSe QDs that have a size distribution of 3−4%. The critical parameters that control inter-QD electronic coupling, and hence carrier transport, include interdot distance, QD surface chemistry, the work function and dielectric properties of the matrix containing the QDs, the nature of the QD capping species, QD orientation and packing order, uniformity of QD size distribution, and the crystallinity and perfection of the individual QDs in the array. Several studies of electronic coupling in colloidal QD arrays have been reported.[157−167] If the semiconductor QD cores are surrounded with insulating organic ligands (to aid in solubility and surface passivation) and a large potential barrier exists between the QDs, the electrons and holes remain confined to the QD, and very weak inter-QD electronic communication exists in such arrays. CdSe QDs in close-packed solids showed that significant electronic coupling could occur[161,162] CdSe QD arrays with QD diameters from 35 to 50 Å showed photoconductivity with applied fields attributed to field-enhanced tunneling, and the photocurrent at a fixed field and temperature increased somewhat with smaller QD diameters.[162] InP QDs with

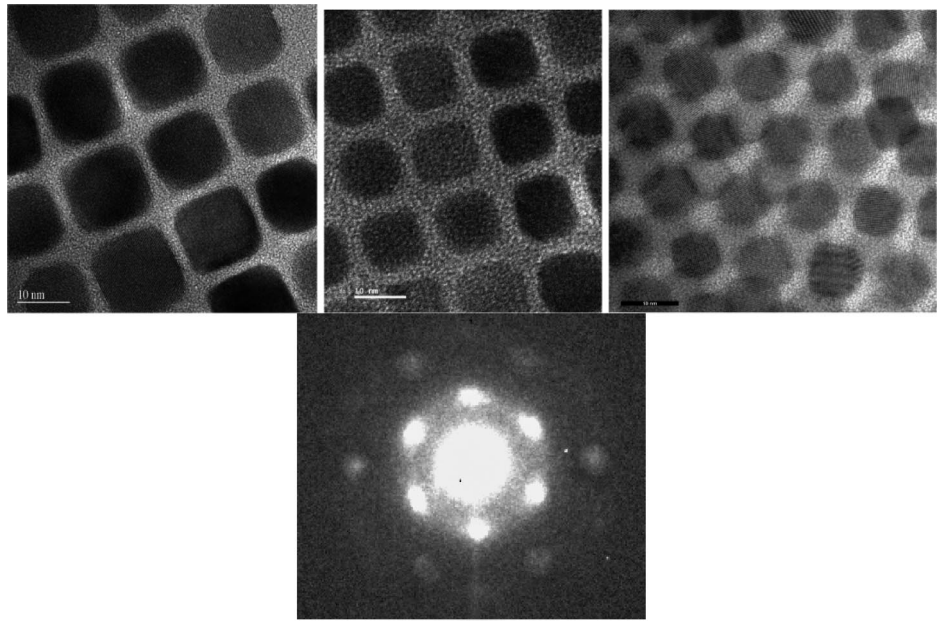

Figure 10. TEM of PbSe and PbTe QD arrays. Left: TEM of arrays of monolayers of cubic QDs of PbSe and PbTe. Right: TEM of multilayers of spherical PbSe QDs showing hexagonal packing. Reprinted with permission from ref 63. Copyright 2006 American Chemical Society.

Treatment	*d(nm)*	ε_s	n_{ave}	μ ($cm_2V^{-1}s^{-1}$)
Oleic Acid	1.8	2	1.57	–
Aniline	0.8	2	2.2	–
Butlyamine	0.4	5.4	2.46	7.4
ethylenediamine	0.4	16	2.62	47.0
Hydrazine	0.25	52	2.69	29.4
NaOH	0.1	1	2.4	35.0

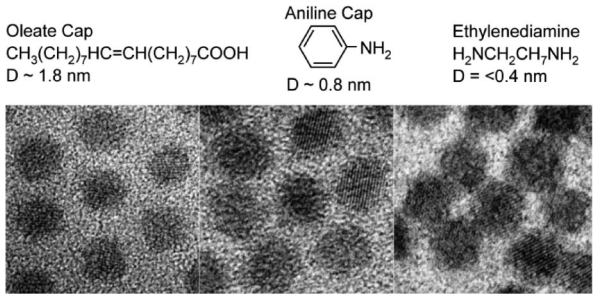

Figure 11. Effect of different chemical treatments of PbSe QD films on interdot distance and carrier mobility as measured by THz spectroscopy from. Reprinted with permission from ref 168. Copyright 2006 American Chemical Society.

diameters 15−23 Å were formed into arrays that showed evidence of electronic coupling[164] based on the differences in the optical spectra of isolated colloidal QDs compared to solid films of QD arrays. Additional work[63,152,163,165−167] on the lead chalcogenides has also shown very good QD array formation with PbSe, PbTe, and PbS QDs. Figure 10 shows arrays of cubic and spherical PbSe and PbTe QDs that show local hexagonal order. The PbSe and PbS QDs films can be converted to conducting n-and p-type films upon treatment with various chemical reagents after film formation. The reagents used have been a variety of very short amine,[166,168,169] thiol,[20,170,171] and carboxylic acids[172] usually diluted in acetonitrile or ethanol; they strip off the organic ligands of the as-made QDs to varying degrees and change the inter-QD distance (see Figure 11) and the corresponding charge mobility as measured by either THz spectroscopy or FET DC conductivity. As discussed below, the 1,2-ethanedithiol (EDT) treatment can be used to make films which produce a well-characterized Schottky junction between the QD film and a metal contact, and it then becomes possible to fabricate a QD solar cell that exhibits a very high photocurrent and significant power conversion efficiency.

Thus, electronic coupling between QDs can take place, and the strength of the electronic coupling increases with decreasing QD diameter and decreasing interdot distance. When the interdot distance in solid QD arrays is large, the QDs maintain their individual identity and their isolated electronic structure, and the array behaves as an insulator. Quantum mechanical coupling becomes important when the potential barrier and distance between the dots is small. A recent paper has shown the dependence of the mobility in PbS and PbSe films on the spacing of the QDs as determined by ligand molecule length.[170] The mobility follows a predicted exponential decay based on the separation of the QDs and the limit of small spacing shows mobilities on the order of 1−10 $cm^2\ V^{-1}\ s^{-1}$. A theoretical study on Si QD arrays showed that for small interdot distances in either a perfect superlattice or in disordered arrays, one can expect the formation of delocalized, extended states from the discrete set of electron and/or hole levels present in the individual QDs.[173] This effect is a 3D analogue to the formation of minibands in a one-dimensional superlattice of quantum wells[174] except that resonant coupling is not as important in the QD arrays. Randomly arranged QDs in a disordered array show the coexistence of both discrete (localized) and bandlike (delocalized) states,[173] and transitions are possible from completely localized electron states to a mixture of localized and delocalized states. The possible mechanisms of transport in QD arrays include nonresonant tunneling, field-assisted tunneling, and hopping. It has been shown that the theory of variable range hopping well describes the temperature dependent transport in PbS and PbSe QD solids[163,166] as well as other similar materials.[175,176]

5.1. MEG in PbSe QD Arrays

Another result of studies of PbSe QD arrays was that the magnitude of the MEG QY was strongly dependent

upon the chemical treatments the arrays were exposed to after array formation.[152] Four different chemical treatments were applied to PbSe QD arrays with QD diameters of 3.7 and 7.4 nm: (1) ethanedithiol, (2) methylamine/ethyl alcohol (me EtOH), (3) hydrazine/acetonitrile (hy ACN), and (4) EtOH. The results were QYs of 100% (no MEG) for EDT treatment for both QD diameters: 150% for me EtOH and hy ACN for both QD diameters and 130% and 225% for EtOH for QD diameters of 3.7 and 7.4 nm, respectively. For untreated PbSe QD films the QYs were 150% and 220% for QD diameters of 3.7 and 7.4 nm, respectively. These experiments show that surface chemistry plays a critical role in determining MEG QYs, as might be expected because surface atoms comprise from 20 to 30% of the atoms in the QD and have an influence on hot exciton relaxation dynamics.

For high efficiency in certain MEG QD solar cell designs, the QDs must be electronically coupled such that charge separation of the exciton occurs on a time scale longer than MEG ($\sim 10^{-13}$ s) but shorter than the biexciton lifetime ($\sim 10^{-10}$ s). The separated charges must then drift and/or diffuse to the electrodes before recombining. In potential QD device geometries,[21] a 3D QD film can form the light-absorbing component of a Schottky or p−n junction heterostructure in which extended states, formed from the coupled QDs, allow for the delocalized photogenerated carriers to traverse the film and reach the contacts or interface. Exchanging bulky capping ligands used in the QD synthesis with shorter molecules after film formation can dramatically increase the carrier mobility of QD films[63,167,177−179] by reducing the interdot spacing[180] while retaining relatively highly passivated surfaces. Distinct excitonic features are still evident in the optical and electro-optic properties of these electronically coupled QD arrays. While this type of close electronic coupling is necessary for the efficient extraction of carriers from a film, it is critical to determine if MEG is preserved in such QD films and to understand how the reduced quantum confinement of the excitons affects the MEG quantum yield (QY).

As for isolated QDs, the decay dynamics of single excitons in the QD films is first determined by photoexciting below the threshold energy for MEG and then the films are excited above the threshold to obtain the information on exciton decay dynamics to determine the MEG QY. This method of determining MEG QY via TA relies on the multiexciton Auger recombination being much faster than single exciton recombination rates. A second, simpler analysis can be used[63,139,146,181] to deduce exciton generation efficiency. The ratio of the normalized change in transmission soon after the excitation pulse (3 ps) to that after all Auger recombination is complete (750 ps) is plotted versus photon fluence, and the following eq 2 can be fitted to the data:

$$R_{\mathrm{pop}} = \frac{\left(\frac{\Delta T}{T_0}\right)_{t=3\mathrm{ps}}}{\left(\frac{\Delta T}{T_0}\right)_{t=750\mathrm{ps}}} = \frac{J_0 \cdot \sigma \cdot \mathrm{QY} \cdot \delta}{1 - \exp(-J_0 \cdot \sigma)} \qquad (2)$$

where R_{pop} is defined as the ratio of exciton populations at 3 and 750 ps after excitation, J_0 is the photon fluence, σ is the absorbance cross section at the pump wavelength, QY is the number of excitons created per excited QD, and δ is the decrease in single exciton population over the time frame of the experiment. This analysis technique not only provides a reliable way to accurately determine the QY of exciton generation, it also enables the direct determination of the absorption cross section (σ) of the QDs in the films at the pump wavelength. Additionally, because the MEG QY is determined by fitting the R_{pop} as J_0 decreases, ultra low photon fluences reduce the possibility of charging effects and false MEG QY values.

Using this procedure, the MEG efficiency was measured in an untreated and an electronically coupled film compared with that of a solution of QDs in TCE from the same synthesis (see Figure 12). The QY can be obtained by calculating the ratio of the QY from the fits above and below the MEG-threshold pumping conditions (see Figure 12). In the sub-MEG-threshold case, a fit of eq 2 is applied where only σ and δ vary and the QY is assumed to be 100%. Above the MEG threshold (top lines in Figure 12), δ is fixed at its sub MEG-threshold value while the QY is allowed to vary. The best-fit value for the QY was found to be 148% at $\sim 4E_g$ for the QDs in TCE as well as in the untreated film and corresponds to the overall average efficiency of exciton generation in an excited QD. The coupled film has an exciton generation efficiency of 164% at $\sim 4E_g$. The QY for the films used in this work is plotted in Figure 13 along with previously reported[138] values for PbSe QDs in solution versus energy gap multiple. The QY results for coupled QD films are similar to what has been previously reported for isolated dots suspended in solvents. These results were all repeated using a smaller size of QDs with larger E_g (0.90 eV) from

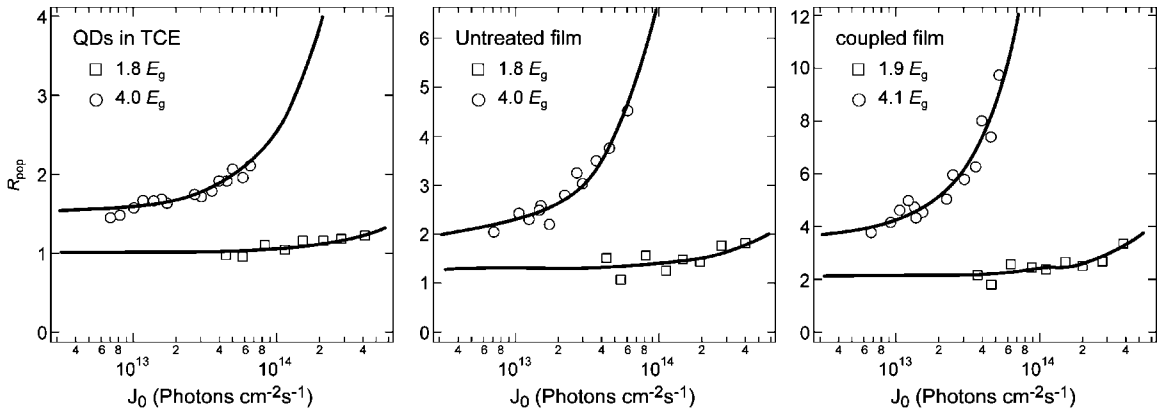

Figure 12. Ratio of exciton population at 3−750 ps (R_{pop}) after excitation with pump energy of $<2E_g$ (squares) and $4E_g$ (circles) vs pump fluence for PbSe QDs in solution (left), in untreated PbSe QD films(middle), and in hydrazine-treated films (right). The fits to these data are described in the text. Reprinted with permission from ref 165. Copyright 2007 American Chemical Society.

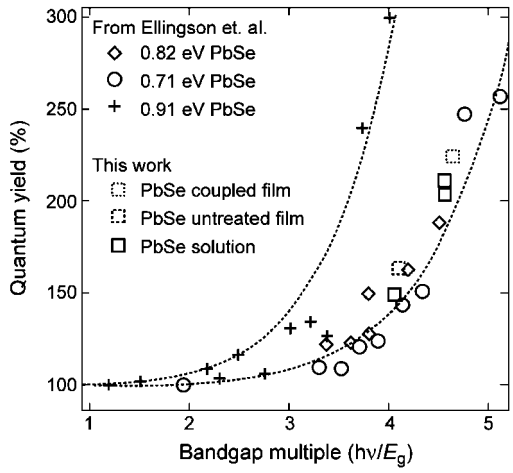

Figure 13. Quantum yield of exciton generation for PbSe QD films and QD solutions. The dotted lines are guides to the eye. Note that the QYs for QDs in solution and untreated films are identical. Reprinted with permission from ref 165. Copyright 2007American Chemical Society.

another synthesis. The QY agrees well with the first sample, and the same trend is observed regarding single exciton and the biexciton lifetimes, aside from the biexciton lifetime scaling with volume.

Thus, after a postfilm-fabrication soak treatment in 1 M hydrazine to electronically couple QDs in QD films, no reduction of MEG efficiency was found in the electronically coupled QD films compared to isolated QDs in solution. This is a particularly interesting and important result because one might expect that in QD arrays exhibiting appreciable electron delocalization resulting in reasonably good charge carrier transport, the MEG efficiency would be greatly reduced because of the reduction of quantum confinement. Thus, the ability to achieve effective electronic coupling between QDs in a QD film without reduction of MEG is very encouraging for the development of novel high-efficiency solar cells employing close-packed arrays of QDs. A related discovery that was discussed above is that MEG can still be efficient in relatively large QDs of Si (5 nm radii, which is equal to the Bohr radius if Si); this means that while the quantum confinement is not sufficient to produce a large confinement kinetic energy with an attendant large blue-shift, the confinement is still enough to produce efficient MEG because Coulomb coupling is still significantly strong.

6. Applications: Quantum Dot Solar Cells

The maximum thermodynamic efficiency for the photovoltaic conversion of unconcentrated solar irradiance into electrical free energy in the radiative limit assuming detailed balance and a single threshold absorber was calculated by Shockley and Queisser in 1961[182] to be about 31−33% for materials with bandgaps ranging from 1 to 1.4 eV; this analysis is also valid for the conversion to chemical free energy.[183,184] Because conversion efficiency is one of the most important parameters to optimize for implementing photovoltaic and photoelectrochemical cells on a truly large scale, several schemes for exceeding the Shockley−Queissar (S−Q) limit have been proposed and are under active investigation.[24] These approaches[185] include tandem cells, hot carrier solar cells,[28,29,158] solar cells producing multiple electron−hole pairs per photon through impact ionization,[21,131,186] multiband and impurity solar cells,[24,187] and thermophotovoltaic/thermophotonic cells.[24] Here, we will only discuss hot carrier and impact ionization solar cells and the effects of size quantization on the carrier dynamics that control the probability of these processes.

The solar spectrum contains photons with energies ranging from about 0.5 to 3.5 eV. Photons with energies below the semiconductor band gap are not absorbed, while those with energies above the band gap create hot electrons and holes with a total excess kinetic energy equal to the difference between the photon energy and the band gap. The initial temperature can be as high as 3000 K with the lattice temperature at 300 K.

A major factor limiting the conversion efficiency in single band gap cells to 31% is that the absorbed photon energy above the semiconductor band gap is lost as heat through electron−phonon scattering and subsequent phonon emission as the carriers relax to their respective band edges (bottom of conduction band for electrons and top of valence for holes). The main approach to reducing this loss in efficiency has been to use a stack of cascaded multiple p−n junctions with band gaps better matched to the solar spectrum; in this way, higher energy photons are absorbed in the higher band gap semiconductors and lower energy photons in the lower band gap semiconductors, thus reducing the overall heat loss due to carrier relaxation via phonon emission. In the limit of an infinite stack of band gaps perfectly matched to the solar spectrum, the ultimate conversion efficiency at one sun intensity can increase to about 66%.

Another approach to increase the conversion efficiency of photovoltaic cells by reducing the loss caused by the thermal relaxation of photogenerated hot electrons and holes is to utilize the hot carriers before they relax to the band edge via phonon emission.[118] There are two fundamental ways to utilize the hot carriers for enhancing the efficiency of photon conversion. One way produces an enhanced photovoltage, and the other way produces an enhanced photocurrent. The former requires that the carriers be extracted from the photoconverter before they cool,[28,29] while the latter requires the energetic hot carriers to produce a second (or more) electron−hole pair through impact ionization,[131,186] a process that is the inverse of an Auger process whereby two electron−hole pairs recombine to produce a single highly energetic electron−hole pair. To achieve the former, the rates of photogenerated carrier separation, transport, and interfacial transfer across the contacts to the semiconductor must all be fast compared to the rate of carrier cooling.[28,30,77,188] The latter requires that the rate of impact ionization (i.e., inverse Auger effect) be greater than the rate of carrier cooling and other relaxation processes for hot carriers.

Hot electrons and hot holes generally cool at different rates because they generally have different effective masses; for most inorganic semiconductors, electrons have effective masses that are significantly lighter than holes and consequently cool more slowly. Another important factor is that hot carrier cooling rates are dependent upon the density of the photogenerated hot carriers (viz, the absorbed light intensity).[73,75,189] Here, most of the dynamical effects we will discuss are dominated by electrons rather than holes; therefore, we will restrict our discussion primarily to the relaxation dynamics of photogenerated electrons.

For QDs, one mechanism for breaking the phonon bottleneck that is predicted to slow carrier cooling in QDs and hence allow fast cooling is an Auger process. Here, a hot electron can give its excess kinetic energy to a thermal-

ized hole via an Auger process, and then the hole can then cool quickly because of its higher effective mass and more closely spaced quantized states. However, if the hole is removed from the QD core by a fast hole trap at the surface, then the Auger process is blocked and the phonon bottleneck effect can occur, thus leading to slow electron cooling. This effect was first shown for CdSe QDs;[88,190] it has now also been shown for InP QDs, where a fast hole trapping species (Na biphenyl) was found, to slow the electron cooling to about 3−4 ps.[190,191] This is to be compared to the electron cooling time of 0.3 ps for passivated InP QDs without a hole trap present and thus where the holes are in the QD core and able to undergo an Auger process with the electrons.[190,191]

6.1. Quantum Dot Solar Cell Configurations

The two fundamental pathways for enhancing the conversion efficiency (increased photovoltage[28,29] or increased photocurrent[131,186]) can be accessed, in principle, in three different QD solar cell configurations; these configurations are shown in Figure 14, and they are described below. However, it is emphasized that these potential high efficiency configurations are theoretical and there are no experimental results yet that demonstrate actual enhanced power conversion efficiencies in QD solar cells over present-day solar cells in any of these systems.

6.1.1. Photoelectrodes Composed of Quantum Dot Arrays

In this configuration (Figure 14), the QDs are formed into an ordered 3-D array with inter-QD spacing sufficiently small such that strong electronic coupling occurs to allow long-range electron transport. This configuration was discussed above in section 6. If the QDs have the same size and are aligned, then this system is a 3-D analogue to a 1-D superlattice and the miniband structures formed therein.[118] The moderately delocalized but still quantized 3-D states could be expected to produce MEG. Also, the slower carrier cooling and delocalized electrons could permit the transport and collection of hot carriers to produce a higher photopotential in a PV or photoelectrochemical cell.

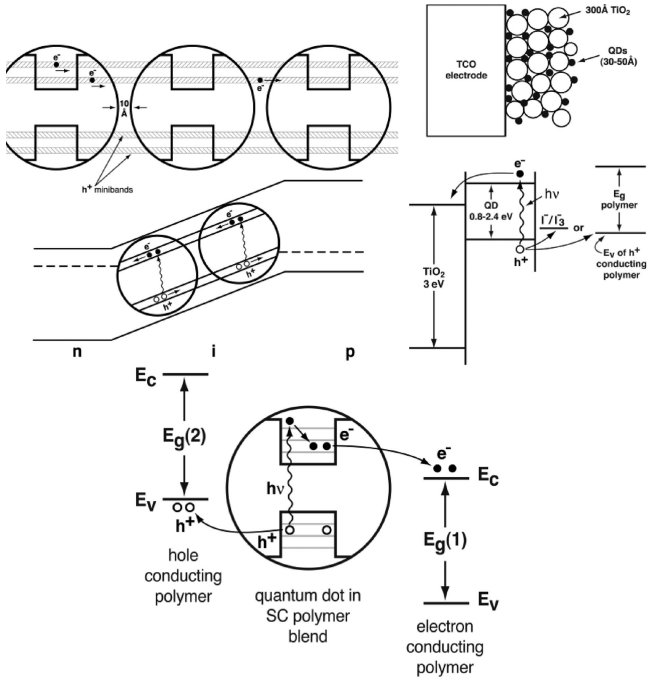

Figure 14. Three different generic QD Solar Cell Configurations. Reprinted with permission from ref 21. Copyright 2002 North Holland.

Significant progress has been made in forming 3-D arrays of both colloidal[33] and epitaxial[70] IV−VI, II−VI, and III−V QDs. The former two systems have been formed via evaporation, crystallization, or self-assembly of colloidal QD solutions containing a reasonably uniform QD size distribution. Although the process can lead to close-packed QD films, they exhibit a significant degree of disorder. Concerning the III−V materials, arrays of epitaxial QDs have been formed by successive deposition of epitaxial QD layers; after the first layer of epitaxial QDs is formed, successive layers tend to form with the QDs in each layer aligned on top of each other.[70,192] Theoretical and experimental studies of the properties of QD arrays are currently under way. Major issues are the nature of the electronic states as a function of interdot distance, array order vs disorder, QD orientation and shape, surface states, surface structure/passivation, and surface chemistry. Transport properties of QD arrays are also of critical importance, and they are under investigation.

6.1.2. Quantum Dot-Sensitized Nanocrystalline TiO_2 Solar Cells

This configuration (Figure 14) is a variation of a recent promising new type of photovoltaic cell that is based on dye-sensitization of nanocrystalline TiO_2 layers.[193−195] In this latter PV cell, dye molecules are chemisorbed onto the surface of 10−30 nm size TiO_2 particles that have been sintered into a highly porous nanocrystalline 10−20 μm TiO_2 film. Upon photoexcitation of the dye molecules, electrons are very efficiently injected from the excited state of the dye into the conduction band of the TiO_2, affecting charge separation and producing a photovoltaic effect.

For the QD-sensitized cell, QDs are substituted for the dye molecules; they can be adsorbed from a colloidal QD solution[196] or produced in situ.[197−200] Successful PV effects in such cells have been reported for several semiconductor QDs including InP, InAs, CdSe, CdS, and PbS.[196−200] Possible advantages of QDs over dye molecules are the tunability of optical properties with size and better heterojunction formation with solid hole conductors. Also, as discussed here, a unique potential capability of the QD-sensitized solar cell is the production of quantum yields greater than one by MEG; a recent study has reported for the first time significant MEG quantum yields in a photoelectrochemical cell utilizing a QD-sensitized single crystal TiO_2 photocathode.[201] Efficient MEG effects in QD-sensitized solar cells could produce higher conversion efficiencies than are possible with dye-sensitized solar cells.

6.1.3. Quantum Dots Dispersed in Organic Semiconductor Polymer Matrices

Recently, photovoltaic effects have been reported in structures consisting of QDs forming intimate junctions with organic semiconductor polymers. In one configuration, a disordered array of CdSe QDs is formed in a hole-conducting polymer, MEH-PPV {poly[2-methoxy,5-(2′-ethyl)-hexyloxy-*p*-phenylenevinylene]}.[202] Upon photoexcitation of the QDs, the photogenerated holes are injected into the MEH-PPV polymer phase and are collected via an electrical contact to the polymer phase. The electrons remain in the CdSe QDs and are collected through diffusion and percolation in the nanocrystalline phase to an electrical contact to the QD

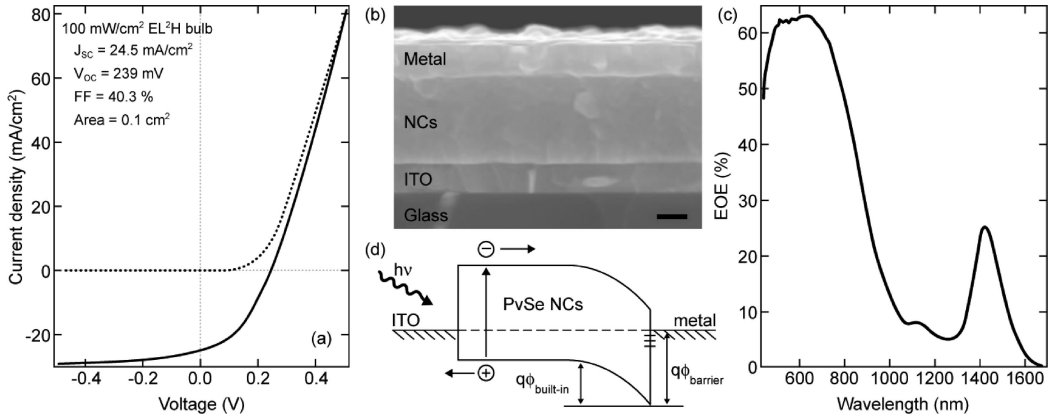

Figure 15. Structure, performance, and schematic diagram of the PbSe QD solar cell: (a) Current−voltage characteristics of a representative cell in the dark and under 100 ± 5 mW cm^{-2} simulated sunlight from an ELH tungsten halogen bulb (E_g of NCs = 0.9 eV). Correcting for the mismatch between the ELH and AM1.5G spectra yields J_{SC} = 21.4 mA cm^{-2} and an overall efficiency of 2.1% for this cell under 100 mW cm^{-2} AM1.5G illumination. The J_{SC} and V_{OC} show the usual linear and logarithmic dependence on light intensity. (b) Scanning electron microscopy (SEM) cross-section of the ITO/NC film/metal device stack. The metal is 20 nm Ca/100 nm Al. The scale bar represents 100 nm. (c) External quantum efficiency (EQE) of a different device with a 140 nm thick film (E_g = 0.95 eV). The first exciton transition of the NC film is seen at 1424 nm. Integrating the product of the EQE and the AM1.5G spectrum from 350−1700 nm yields J_{SC} 18.4 mA cm^{-2}. (d) Proposed equilibrium band diagram. Light is incident through the ITO and band bending occurs at the interface between the NCs and evaporated negative electrode. Reprinted with permission from ref 219. Copyright 2008 American Chemical Society.

network. Initial results show relatively low conversion efficiencies,[202,203] but improvements have been reported with rod-like CdSe QD shapes[204] embedded in poly(3-hexylthiophene) (the rod-like shape enhances electron transport through the nanocrystalline QD phase) and recently[205] with newer polymers (PCDTBT, Konarka) that allow for better electrical properties (3.13%, NREL certified). In another configuration,[206] a polycrystalline TiO_2 layer is used as the electron conducting phase, and MEH-PPV is used to conduct the holes; the electron and holes are injected into their respective transport mediums upon photoexcitation of the QDs.

A variation of these configurations is to disperse the QDs into a blend of electron and hole-conducting polymers (Figure 14c).[207] This scheme is the inverse of light emitting diode structures based on QDs.[208−212] In the PV cell, each type of carrier-transporting polymer would have a selective electrical contact to remove the respective charge carriers. A critical factor for success is to prevent electron−hole recombination at the interfaces of the two polymer blends; prevention of electron−hole recombination is also critical for the other QD configurations mentioned above.

All of the possible QD−organic polymer photovoltaic cell configurations would benefit greatly if the QDs can produce multiple electron−hole pairs by the MEG process[201] This is also true for all the QD solar cell systems described above. The most important process in all the QD solar cells for reaching very high conversion efficiency is the multiple electron−hole pair production in the photoexcited QDs; the various cell configurations simply represent different modes of collecting and transporting the photogenerated carriers produced in the QDs.

6.2. Schottky Junction and p−n Junction Solar Cells Based on Films of QD Arrays

To date, multiple exciton generation has been studied in NCs of the lead salts,[63,138,139,165] InAs,[144,150,213] CdSe,[148,181] and Si[146] using several time-resolved and quasi-CW spectroscopies; negative results were recently reported for InAs[150] and CdSe.[148] It is therefore important to establish whether significant MEG photocurrent can be collected from a NC solar cell, but this is complicated by the poor external quantum efficiencies (EQEs) of existing NC devices.[213−218] A simple, all-inorganic metal/NC/metal sandwich cell has been reported[219] that produces a large short-circuit photocurrent (∼25 mA cm^{-2}) by way of a Schottky junction at the negative electrode. The PbSe NC film, deposited via layer-by-layer (LbL) dip coating, yields an EQE of 55−65% in the visible and up to 25% in the infrared region of the solar spectrum, with an AM1.5G power conversion efficiency of 2.1%. This NC device produces one of the largest short-circuit currents of any nanostructured solar cell, without the need for sintering, superlattice order or separate phases for electron and hole transport, but MEG was not confirmed in this cell.

Figure 15 shows the structure, current−voltage performance, EQE spectrum, and proposed band diagram of the device. Device fabrication consists of depositing a 60−300 nm thick film of monodisperse, spheroidal PbSe NCs onto patterned indium tin oxide (ITO) coated glass using a layer-by-layer (LbL) dip coating method, followed by evaporation of a top metal contact. In this LbL method,[219] a layer of NCs is deposited onto the ITO surface by dip coating from a hexane solution and then washed in 0.01 M 1,2-ethanedithiol in acetonitrile to remove the electrically insulating oleate ligands that originally solubilizes the NCs. Large-area, crack-free, and mildly conductive ($\sigma = 5 \times 10^{-5}$ S cm^{-1}) NC films result. The NCs pack randomly in the films, are partially coated in adsorbed ethanedithiolate, and show p-type DC conductivity under illumination.[219] X-ray diffraction and optical absorption spectroscopy established that the NCs neither ripen nor sinter in response to EDT exposure. It was found that using methylamine instead of EDT yields similar device performance. Working devices were also fabricated from PbS and CdSe NCs, which indicates that the approach adopted here is not restricted to EDT-treated PbSe NCs and that it should be possible to improve cell efficiency by engineering the surface of the NCs to attain longer carrier diffusion lengths. Multiple lines of evidence suggest that the photogenerated carriers in the device are separated by a Schottky barrier at the evaporated metal contact and also recently observed in films of PbS NCs.[220] However, changing

the contact metal from gold to calcium ($|\Delta\phi_m| = 2.3$ eV) results in only a 0.15 V increase in V_{OC}, which suggests that the surface Fermi level is pinned and the barrier height is relatively independent of the metal. Schottky barrier formation is often due to defects formed at an interface by deposition of a metal.[221] Direct evidence for the Schottky junction was obtained by capacitance−voltage ($C-V$) measurements on complete cells.[219]

The location of the Schottky junction was determined by comparing the EQE spectra from cells of different thickness.[219] It was found that the EQE decreased markedly in the blue region of the spectrum as the thickness of the NC film increased from 65 to 400 nm. This falloff in the blue indicates that the charge-separating junction occurs at the back contact, at the interface between the NC film and the evaporated metal electrode. Because thicker devices have a wider field-free region near the ITO, blue photons, which are absorbed nearer the front of the cell ($1/\alpha = 75-100$ nm at $\lambda = 450$ nm), contribute progressively less to the photocurrent than do red photons, which penetrate closer to the depletion layer near the back contact.

This film concept has been further extended into heterojunction devices with the QD layer acting as the absorber. ZnO was used to first demonstrate that the polarity of charge can be inverted and the junction be relocated to the incident side of the device.[222] Groups at Cornell[223] have employed ZnO to increase the V_{oc} of the device, yet only smaller PbSe NCs with a large bandgap can effectively inject charge across the PbSe/ZnO barrier. Recent results at NREL show a much enhanced air stability of devices when employing ZnO below a PbS layer deposited in air with Au as the back electrode. In this configuration, the device yields a 3% (NREL certified) efficiency that is stable in air for months.[224]

7. Conclusion

Many classes of semiconductor quantum dots (also called nanocrystals) have been synthesized, including groups II−VI, III−V, IV−VI, IV, and their alloys, various intergroup and intragroup core−shell configurations, and various nanocrystal shapes. Recent research has improved upon the nanocrystal syntheses regarding more friendly "green" chemistry, better size distributions and stability, lower synthesis temperatures, and more uniform nanocrystals in general.

The application of QDs in solar photon conversion devices (solar cells for photovoltaics and solar fuels) to enhance their conversion efficiencies is a promising and increasingly active field of research. Such cells are termed "future generation" or in the case of PV: "third-generation" solar cells. One approach to enhance efficiency in QD-based PV cells compared to conventional bulk semiconductor-based PV is to create efficient multiple exciton generation from a large fraction of the photons in the solar spectrum. Enhanced MEG quantum yields have now been confirmed by several groups in isolated colloidal QDs of PbSe, PbS, PbTe, Si, InP, CdTe, core−shell CdSe/CdTe, and in QD arrays of PbS, PbTe, and PbSe. It is noted that MEG has also been reported in single-wall carbon nanotubes.

The most common method for determining the MEG QY has been ps to ns time-resolved spectroscopy (transient absorption, bleaching, photoluminescence, and THz); steady-state photocurrent spectroscopy measurements are also under study. Discrepancies in the literature for reported MEG QY values for PbSe and CdSe are explained by variations in the surface chemistry of the QDs and in some cases the effects of charging of QDs when photogenerated electrons or holes are trapped at the surface producing a charged QD core. After accounting for these variations and effects, MEG has been confirmed in the various QD materials discussed here and for these materials have threshold photon energies for MEG ranging from $2.1E_g$ to $3E_g$, and total QYs at $3.0E_g$, for example, ranging from 120% to 200%. With these MEG characteristics, the improvement in PV power conversion efficiency is relatively minor; to achieve significant increased power conversion efficiency, the MEG threshold needs to be close to $2E_g$ with a sharp increase in QY that reaches ~200% at ~$2.1E_g$ to 2.5 E_g and ~300% at $3E_g$ to $3.5E_g$.

In summary, three generic types of QD solar cells that could utilize MEG to enhance conversion efficiency can be defined: (1) photoelectrodes composed of QD arrays that form either Schottky junctions with a metal layer, a hetero p−n junction with a second NC semiconductor layer, or the i-region of a p-i-n device, (2) QD-sensitized nanocrystalline TiO_2 films, and (3) QDs dispersed into a multiphase mixture of electron- and hole-conducting matrices, such as C60 and hole conducting polymers (like polythiophene or MEH-PPV), respectively. Additional research and understanding is required to realize the potential of MEG to significantly enhance solar cell performance.

8. Acknowledgments

We acknowledge important contributions to the work generated here from: O. I. Micic (deceased), J. E. Murphy, M. C. Hanna, P. Yu, Sasha Efros, and Andrew Shabaev. All authors were supported by the U.S. Department of Energy, Office of Science, Office of Basic Energy Sciences, Division of Chemical Sciences, Geosciences, and Biosciences, Solar Photochemistry Program.

9. Note Added after ASAP Publication

This article published on October 14, 2010. A recent publication (Beard, M. C.; Midgett, A. G.; Hanna, M. C.; Luther, J. M.; Hughes, B. K.; Nozik, A. J. *Nano Lett*., **2010**, *10*, 3019) has shown that the scatter in MEG QYs vs photon energy, shown typically in Figure 6, can be eliminated by flowing or stirring the samples to avoid complications due to photocharging. Experiments at NREL and LANL on the same colloidal QD samples, using both TA and transient PL, converged to the same values. Also, ref 154 has been updated (*J. Phys. Chem. C* **2010**, *114*, 17486). The new version reposted ASAP on October 20, 2010.

10. References

(1) Wang, N.; Cai, Y.; Zhang, R. Q. *Mater. Sci. Eng., R* **2008**, *60*, 1.
(2) Sham, T. K. *Int. J. Nanotechnol.* **2008**, *5*, 1194.
(3) Goncher, G.; Solanki, R. *Proc. SPIE Int. Soc. Opt. Eng.* **2008**, *70470L*, 14.
(4) Abdelsayed, V.; Panda, A. B.; Glaspell, G. P.; El Shall, M. S. In *Nanoparticles: Synthesis, Stabilization, Passivation, and Functionalization*; American Chemical Society: Washington, DC, 2008.
(5) Baca, A. J.; Ahn, J. H.; Sun, Y. G.; Meitl, M. A.; Menard, E.; Kim, H. S.; Choi, W. M.; Kim, D. H.; Huang, Y.; Rogers, J. A. *Angew. Chem., Int. Ed.* **2008**, *47*, 5524.
(6) Kislyuk, V. V.; Dimitriev, O. P. *J. Nanosci. Nanotechnol.* **2008**, *8*, 131.
(7) Yu, D. P. In *Nanowires and Nanobelts*; Wang, Z. L., Ed.; Kluwer Academic Publishers: Norwell, MA, 2003; Vol. 1.
(8) Guo, Q.; Kim, S. J.; Kar, M.; Shafarman, W. N.; Birkmire, R. W.; Stach, E. A.; Agrawal, R.; Hillhouse, H. W. *Nano Lett.* **2008**, *8*, 2982–2987.

(9) Chen, J. X.; Liao, W. S.; Chen, X.; Yang, T. L.; Wark, S. E.; Son, D. H.; Batteas, J. D.; Cremer, P. S. *ACS Nano* **2009**, *3*, 173–180.
(10) Lee, C. H.; Liu, C. W.; Chang, H. T.; Lee, S. W. *J. Appl. Phys.* **2010**, *107*, 056103/1.
(11) Cho, K. S.; Talapin, D. V.; Gaschler, W.; Murray, C. B. *J. Am. Chem. Soc.* **2005**, *127*, 7140.
(12) Manna, L.; Scher, E. C.; Alivisatos, A. P. *J. Am. Chem. Soc.* **2000**, *122*, 12700.
(13) Manna, L.; Milliron, D. J.; Meisel, A.; Scher, E. C.; Alivisatos, A. P. *Nature Mater.* **2003**, *2*, 382.
(14) Huynh, W. U.; Dittmer, J. J.; Alivisatos, A. P. *Science* **2002**, *295*, 2425.
(15) Nozik, A. J. *Inorg. Chem.* **2005**, *44*, 6893.
(16) Nozik, A. J. *Chem. Phys. Lett.* **2008**, *457*, 3.
(17) Beard, M. C.; Ellingson, R. J. *Laser Photonics Rev.* **2008**, *2*, 377.
(18) Hillhouse, H. W.; Beard, M. C. *Curr. Opin. Colloid Interface Sci.* **2009**, *14*, 245.
(19) *Nanocrystal Quantum Dots: Synthesis and Electronic and Optical Properties*, 2nd ed.; Klimov, V. I., Ed.; CRC Press, Taylor & Francis Group: Boca Raton, FL, 2010.
(20) Luther, J. M.; Law, M.; Song, Q.; Perkins, C. L.; Beard, M. C.; Nozik, A. J. *ACS Nano* **2008**, *2*, 271.
(21) Nozik, A. J. *Physica E* **2002**, *14*, 115.
(22) Tian, B.; Kempa, T. J.; Lieber, C. M. *Chem. Soc. Rev.* **2009**, *38*, 16.
(23) Law, M.; Greene, L. E.; Johnson, J. C.; Saykally, R.; Yang, P. D. *Nature Mater.* **2005**, *4*, 455.
(24) Green, M. A. *Third Generation Photovoltaics*; Bridge Printery: Sydney, Australia, 2001.
(25) *Next Generation Photovoltaics: High Efficiency through Full Spectrum Utilization*; Martí, A., Luque, A., Eds.; Institute of Physics: Bristol, UK, 2003.
(26) Williams, F.; Nozik, A. J. *Nature* **1978**, *271*, 137.
(27) Nozik, A. J. *Annu. Rev. Phys. Chem.* **1978**, *29*, 189.
(28) Boudreaux, D. S.; Williams, F.; Nozik, A. J. *J. Appl. Phys.* **1980**, *51*, 2158.
(29) Ross, R. T.; Nozik, A. J. *J. Appl. Phys.* **1982**, *53*, 3813.
(30) Williams, F. E.; Nozik, A. J. *Nature* **1984**, *311*, 21.
(31) Steigerwald, M. L.; Brus, L. E. *Annu. Rev. Mater. Sci.* **1989**, *19*, 471.
(32) Bawendi, M. G.; Steigerwald, M. L.; Brus, L. E. *Annu. Rev. Phys. Chem.* **1990**, *41*, 477.
(33) Murray, C. B.; Kagan, C. R.; Bawendi, M. G. *Annu. Rev. Mater. Sci.* **2000**, *30*, 545.
(34) Efros, A. L.; Rosen, M. *Annu. Rev. Mater. Sci.* **2000**, *30*, 475.
(35) Kash, K. *J. Lumin.* **1990**, *46*, 69.
(36) *Semiconductor and Metal Nanocrystals: Synthesis and Electronic and Optical Properties*; Klimov, V. I., Ed.; Marcel Dekker, Inc.: New York, 2004; Vol. 87.
(37) In *Semiconductor and Metal Nanocrystals: Synthesis and Electronic and Optical Properties*; Klimov, V., Ed.; Marcel Dekker, Inc.: New York, 2003.
(38) Mićić, O. I.; Nozik, A. J. In *Handbook of Nanostructured Materials and Nanotechnology*; Nalwa, H. S., Ed.; Academic Press: San Diego, 2000; Vol. 3.
(39) Peyghambarian, N.; Tajalli, H. *Glass Sci. Technol.* **1997**, 313.
(40) Henneberger, F., Puls, J. In *Optics of Semiconductor Nanostructures*; Henneberger, F., Schmitt-Rink, S., Goebel, E. O., Ed.; Akademie-Verlag: Berlin, 1993.
(41) Peng, X. G. *Chem.—A Eur. J.* **2002**, *8*, 335.
(42) Peng, X. G. *Nano Res.* **2009**, *2*, 425.
(43) Murray, C. B.; Sun, S.; Gaschler, W.; Doyle, H.; Betley, T. A.; Kagan, C. R. *IBM J. Res. Dev.* **2001**, *45*, 47–56.
(44) Chen, Y. F.; Kim, M.; Lian, G.; Johnson, M. B.; Peng, X. G. *J. Am. Chem. Soc.* **2005**, *127*, 13331.
(45) Yang, Y. A.; Wu, H. M.; Williams, K. R.; Cao, Y. C. *Angew. Chem., Int. Ed.* **2005**, *44*, 6712.
(46) Xie, R. G.; Peng, X. G. *Angew. Chem., Int. Ed.* **2008**, *47*, 7677.
(47) Alivisatos, A. P. *Science* **1996**, *271*, 933–937.
(48) Reiss, P. In *Semiconductor Nanocrystals Quantum Dots*; Rogach, A., Ed.; Springer: New York, 2008; Vol. XI.
(49) Peng, Z. A.; Peng, X. G. *J. Am. Chem. Soc.* **2001**, *123*, 183.
(50) Xie, R.; Battaglia, D.; Peng, X. *J. Am. Chem. Soc.* **2007**, *129*, 15432.
(51) Crouch, D.; Norager, S.; O'Brien, P.; Park, J. H.; Pickett, N. *Philos. Trans. R. Soc. London, Ser. A* **2003**, *361*, 297.
(52) Green, M. *Curr. Opin. Solid State Mater. Sci.* **2002**, *6*, 355.
(53) Esteves, A. C. C.; Trindade, T. *Curr. Opin. Solid State Mater. Sci.* **2002**, *6*, 347.
(54) Grieve, K.; Mulvaney, P.; Grieser, F. *Curr. Opin. Colloid Interface Sci.* **2000**, *5*, 168.
(55) El-Sayed, M. A. *Acc. Chem. Res.* **2004**, *37*, 326.
(56) Stubbs, S. K.; Hardman, S. J. O.; Graham, D. M.; Spencer, B. F.; Flavell, W. R.; Glarvey, P.; Masala, O.; Pickett, N. L.; Binks, D. J. *Phys. Rev. B* **2010**, 81.
(57) Gachet, D.; Avidan, A.; Pinkas, I.; Oron, D. *Nano Lett.* **2010**, *10*, 164–170.
(58) Weller, H.; Eychmüller, A. In *Semiconductor Nanoclusters*; Kamat, P. V., Meisel, D., Eds.; Elsevier Science BV: Amsterdam, 1997; Vol. 103.
(59) Overbeek, J. T. G. *Adv. Colloid Interface Sci.* **1982**, *15*, 251.
(60) Murray, C. B. Synthesis and Characterization of II-VI Quantum Dots and Their Assembly into 3D Quantum Dot Superlattices. Ph.D. Thesis, Department of Chemistry, Massachusetts Institute of Technology, 1995.
(61) Murray, C. B.; Norris, D. J.; Bawendi, M. G. *J. Am. Chem. Soc.* **1993**, *115*, 8706.
(62) Yu, W. W.; Falkner, J. C.; Shih, B. S.; Colvin, V. L. *Chem. Mater.* **2004**, *16*, 3318.
(63) Murphy, J. E.; Beard, M. C.; Norman, A. G.; Ahrenkiel, S. P.; Johnson, J. C.; Yu, P.; Mićić, O. I.; Ellingson, R. J.; Nozik, A. J. *J. Am. Chem. Soc.* **2006**, *128*, 3241.
(64) Mićić, O. I.; Sprague, J. R.; Curtis, C. J.; Jones, K. M.; Machol, J. L.; Nozik, A. J.; Giessen, H.; Fluegel, B.; Mohs, G.; Peyghambarian, N. *J. Phys. Chem.* **1995**, *99*, 7754.
(65) Mićić, O. I.; Curtis, C. J.; Jones, K. M.; Sprague, J. R.; Nozik, A. J. *J. Phys. Chem.* **1994**, *98*, 4966.
(66) Mićić, O. I.; Sprague, J. R.; Lu, Z.; Nozik, A. J. *Appl. Phys. Lett.* **1996**, *68*, 3150.
(67) Langof, L.; Ehrenfreund, E.; Lifshitz, E.; Mićić, O. I.; Nozik, A. J. *J. Phys. Chem. B* **2002**, *106*, 1606.
(68) Mićić, O. I.; Cheong, H. M.; Fu, H.; Zunger, A.; Sprague, J. R.; Mascarenhas, A.; Nozik, A. J. *J. Phys. Chem. B* **1997**, *101*, 4904.
(69) Petroff, P. M.; Denbaars, S. P. *Superlattices Microstruct.* **1994**, *15*, 15.
(70) *Self-Assembled InGaAs/GaAs Quantum Dots*; Sugawara, M., Ed.; Academic Press: San Diego, 1999; Vol. 60.
(71) Mohan, A.; Gallo, P.; Felici, M.; Dwir, B.; Rudra, A.; Faist, J.; Kapon, E. *Small* **2010**, *6*, 1268.
(72) Nozik, A. J. *Annu. Rev. Phys. Chem.* **2001**, *52*, 193.
(73) Pelouch, W. S.; Ellingson, R. J.; Powers, P. E.; Tang, C. L.; Szmyd, D. M.; Nozik, A. J. *Phys. Rev. B* **1992**, *45*, 1450.
(74) Ulstrup, J.; Jortner, J. *J. Chem. Phys.* **1975**, *63*, 4358.
(75) Rosenwaks, Y.; Hanna, M. C.; Levi, D. H.; Szmyd, D. M.; Ahrenkiel, R. K.; Nozik, A. J. *Phys. Rev. B* **1993**, *48*, 14675.
(76) Pelouch, W. S.; Ellingson, R. J.; Powers, P. E.; Tang, C. L.; Szmyd, D. M.; Nozik, A. J. *SPIE* **1993**, *1677*, 260.
(77) Nozik, A. J.; Boudreaux, D. S.; Chance, R. R.; Williams, F. In *Advances in Chemistry*; Wrighton, M., Ed.; American Chemical Society: Washington, DC, 1980; Vol. 184.
(78) Benisty, H.; Sotomayor-Torres, C. M.; Weisbuch, C. *Phys. Rev. B* **1991**, *44*, 10945.
(79) Bockelmann, U.; Bastard, G. *Phys. Rev. B* **1990**, *42*, 8947.
(80) Bockelmann, U.; Egeler, T. *Phys. Rev. B* **1992**, *46*, 15574.
(81) Benisty, H. *Phys. Rev. B* **1995**, *51*, 13281.
(82) Efros, A. L.; Kharchenko, V. A.; Rosen, M. *Solid State Commun.* **1995**, *93*, 281.
(83) Vurgaftman, I.; Singh, J. *Appl. Phys. Lett.* **1994**, *64*, 232.
(84) Sercel, P. C. *Phys. Rev. B.* **1995**, *51*, 14532.
(85) Inoshita, T.; Sakaki, H. *Phys. Rev. B* **1992**, *46*, 7260.
(86) Inoshita, T.; Sakaki, H. *Phys. Rev. B* **1997**, *56*, R4355.
(87) Padney, A.; Guyot-Sionnest, P. *Science* **2008**, *322*, 929.
(88) Guyot-Sionnest, P.; Shim, M.; Matranga, C.; Hines, M. *Phys. Rev. B.* **1999**, *60*, R2181.
(89) Wang, G.; Fafard, S.; Leonard, D.; Bowers, J. E.; Merz, J. L.; Petroff, P. M. *Appl. Phys. Lett.* **1994**, *64*, 2815.
(90) Mukai, K.; Sugawara, M. *Jpn. J. Appl. Phys.* **1998**, *37*, 5451.
(91) Mukai, K.; Ohtsuka, N.; Shoji, H.; Sugawara, M. *Appl. Phys. Lett.* **1996**, *68*, 3013.
(92) Murdin, B. N.; Hollingworth, A. R.; Kamal-Saadi, M.; Kotitschke, R. T.; Ciesla, C. M.; Pidgeon, C. R.; Findlay, P. C.; Pellemans, H. P. M.; Langerak, C. J. G. M.; Rowe, A. C.; Stradling, R. A.; Gornik, E. *Phys. Rev. B* **1999**, *59*, R7817.
(93) Sugawara, M.; Mukai, K.; Shoji, H. *Appl. Phys. Lett.* **1997**, *71*, 2791.
(94) Heitz, R.; Veit, M.; Ledentsov, N. N.; Hoffmann, A.; Bimberg, D.; Ustinov, V. M.; Kop'ev, P. S.; Alferov, Z. I. *Phys. Rev. B* **1997**, *56*, 10435.
(95) Heitz, R.; Kalburge, A.; Xie, Q.; Grundmann, M.; Chen, P.; Hoffmann, A.; Madhukar, A.; Bimberg, D. *Phys. Rev. B* **1998**, *57*, 9050.
(96) Mukai, K.; Ohtsuka, N.; Shoji, H.; Sugawara, M. *Phys. Rev. B* **1996**, *54*, R5243.
(97) Yu, H.; Lycett, S.; Roberts, C.; Murray, R. *Appl. Phys. Lett.* **1996**, *69*, 4087.
(98) Adler, F.; Geiger, M.; Bauknecht, A.; Scholz, F.; Schweizer, H.; Pilkuhn, M. H.; Ohnesorge, B.; Forchel, A. *J. Appl. Phys.* **1996**, *80*, 4019.

(99) Adler, F.; Geiger, M.; Bauknecht, A.; Haase, D.; Ernst, P.; Dörnen, A.; Scholz, F.; Schweizer, H. *J. Appl. Phys.* **1998**, *83*, 1631.
(100) Brunner, K.; Bockelmann, U.; Abstreiter, G.; Walther, M.; Böhm, G.; Tränkle, G.; Weimann, G. *Phys. Rev. Lett.* **1992**, *69*, 3216.
(101) Kamath, K.; Jiang, H.; Klotzkin, D.; Phillips, J.; Sosnowski, T.; Norris, T.; Singh, J.; Bhattacharya, P. *Inst. Phys. Conf. Ser.* **1998**, *156*, 525.
(102) Gfroerer, T. H.; Sturge, M. D.; Kash, K.; Yater, J. A.; Plaut, A. S.; Lin, P. S. D.; Florez, L. T.; Harbison, J. P.; Das, S. R.; Lebrun, L. *Phys. Rev. B* **1996**, *53*, 16474.
(103) Li, X.-Q.; Nakayama, H.; Arakawa, Y. In *Proceedings of the 24th International Conference on the Physics of Semiconductors*; Gershoni, D., Ed.; World Scientific: Singapore, 1998.
(104) Bellessa, J.; Voliotis, V.; Grousson, R.; Roditchev, D.; Gourdon, C.; Wang, X. L.; Ogura, M.; Matsuhata, H. In *Proceedings of the 24th International Conference on the Physics of Semiconductors*; Gershoni, D., Ed.; World Scientific: Singapore, 1998.
(105) Lowisch, M.; Rabe, M.; Kreller, F.; Henneberger, F. *Appl. Phys. Lett.* **1999**, *74*, 2489.
(106) Gontijo, I.; Buller, G. S.; Massa, J. S.; Walker, A. C.; Zaitsev, S. V.; Gordeev, N. Y.; Ustinov, V. M.; Kop'ev, P. S. *Jpn. J. Appl. Phys.* **1999**, *38*, 674.
(107) Li, X.-Q.; Nakayama, H.; Arakawa, Y. *Jpn. J. Appl. Phys.* **1999**, *38*, 473.
(108) Kral, K.; Khas, Z. *Phys. Status Solidi B* **1998**, *208*, R5.
(109) Klimov, V. I.; McBranch, D. W. *Phys. Rev. Lett.* **1998**, *80*, 4028.
(110) Bimberg, D.; Ledentsov, N. N.; Grundmann, M.; Heitz, R.; Boehrer, J.; Ustinov, V. M.; Kop'ev, P. S.; Alferov, Z. I. *J. Lumin.* **1997**, *72*−*74*, 34.
(111) Woggon, U.; Giessen, H.; Gindele, F.; Wind, O.; Fluegel, B.; Peyghambarian, N. *Phys. Rev. B* **1996**, *54*, 17681.
(112) Grundmann, M.; Heitz, R.; Ledentsov, N.; Stier, O.; Bimberg, D.; Ustinov, V. M.; Kop'ev, P. S.; Alferov, Z. I.; Ruvimov, S. S.; Werner, P.; Gösele, U.; Heydenreich, J. *Superlattices Microstruct.* **1996**, *19*, 81.
(113) Williams, V. S.; Olbright, G. R.; Fluegel, B. D.; Koch, S. W.; Peyghambarian, N. *J. Mod. Opt.* **1988**, *35*, 1979.
(114) Ohnesorge, B.; Albrecht, M.; Oshinowo, J.; Forchel, A.; Arakawa, Y. *Phys. Rev. B* **1996**, *54*, 11532.
(115) Heitz, R.; Veit, M.; Kalburge, A.; Xie, Q.; Grundmann, M.; Chen, P.; Ledentsov, N. N.; Hoffmann, A.; Madhukar, A.; Bimberg, D.; Ustinov, V. M.; Kop'ev, P. S.; Alferov, Z. I. *Physica E* **1998**, *2*, 578.
(116) Li, X.-Q.; Arakawa, Y. *Phys. Rev. B* **1998**, *57*, 12285.
(117) Sosnowski, T. S.; Norris, T. B.; Jiang, H.; Singh, J.; Kamath, K.; Bhattacharya, P. *Phys. Rev. B* **1998**, *57*, R9423.
(118) Miller, R. D. J.; McLendon, G.; Nozik, A. J.; Schmickler, W.; Willig, F. *Surface Electron Transfer Processes*; VCH Publishers: New York, 1995.
(119) Meier, A.; Selmarten, D. C.; Siemoneit, K.; Smith, B. B.; Nozik, A. J. *J. Phys. Chem. B* **1999**, *103*, 2122.
(120) Meier, A.; Kocha, S. S.; Hanna, M. C.; Nozik, A. J.; Siemoneit, K.; Reineke-Koch, R.; Memming, R. *J. Phys. Chem. B* **1997**, *101*, 7038.
(121) Diol, S. J.; Poles, E.; Rosenwaks, Y.; Miller, R. J. D. *J. Phys. Chem. B* **1998**, *102*, 6193.
(122) Kempa, K.; Naughton, M. J.; Ren, Z. F.; Herczynski, A.; Kirkpatrick, T.; Rybczynski, J.; Gao, Y. *Appl. Phys. Lett.* **2009**, *95*, 233121.
(123) Hanna, M. C.; Nozik, A. J. *J. Appl. Phys.* **2006**, *100*, 074510.
(124) Klimov, V. I. *Appl. Phys. Lett.* **2006**, *89*, 123118.
(125) Koc, S. *Czech. J. Phys.* **1957**, *7*, 91.
(126) Vavilov, V. S. *J. Phys. Chem. Solids* **1959**, *8*, 223.
(127) Tauc, J. *J. Phys. Chem. Solids* **1959**, *8*, 219.
(128) Ivakhno, V. N. *Sov. Phys. Solid State* **1972**, *14*, 481.
(129) Christensen, O. *J. Appl. Phys.* **1976**, *47*, 689.
(130) Beattie, A. R. *J. Phys. Chem. Solids* **1962**, *24*, 1049.
(131) Kolodinski, S.; Werner, J. H.; Wittchen, T.; Queisser, H. J. *Appl. Phys. Lett.* **1993**, *63*, 2405.
(132) Baryshev, N. S.; Shchetinin, M. P.; Chashchin, S. P.; Kharionovskii, Y. S.; Aver'yanov, I. S. *Sov. Phys. Semicond.* **1974**, *8*, 192.
(133) Bude, J.; Hess, K. *J. Appl. Phys.* **1992**, *72*, 3554.
(134) Jung, H. K.; Taniguchi, K.; Hamaguchi, C. *J. Appl. Phys.* **1996**, *79*, 2473.
(135) Harrison, D.; Abram, R. A.; Brand, S. *J. Appl. Phys.* **1999**, *85*, 8186.
(136) Wolf, M.; Brendel, R.; Werner, J. H.; Queisser, H. J. *J. Appl. Phys.* **1998**, *83*, 4213.
(137) Shabaev, A.; Efros, A. L.; Nozik, A. J. *Nano Lett.* **2006**, *6*, 2856.
(138) Ellingson, R. J.; Beard, M. C.; Johnson, J. C.; Yu, P.; Mićić, O. I.; Nozik, A. J.; Shabaev, A.; Efros, A. L. *Nano Lett.* **2005**, *5*, 865.
(139) Schaller, R.; Klimov, V. *Phys. Rev. Lett.* **2004**, *92*, 186601.
(140) Trinh, M. T.; Houtepen, A. J.; Schins, J. M.; Hanrath, T.; Piris, J.; Knulst, W.; Goossens, A.; Siebbeles, L. D. A. *Nano Lett.* **2008**, *8*, 1713.
(141) Ji, M. B.; Park, S.; Connor, S. T.; Mokari, T.; Cui, Y.; Gaffney, K. J. *Nano Lett.* **2009**, *9*, 1217.
(142) Schaller, R. D.; Petruska, M. A.; Klimov, V. I. *Appl. Phys. Lett.* **2005**, *87*, 253102.
(143) Schaller, R. D.; Sykora, M.; Jeong, S.; Klimov, V. I. *J. Phys. Chem. B* **2006**, *110*, 25332.
(144) Pijpers, J. J. H.; Hendry, E.; Milder, M. T. W.; Fanciulli, R.; Savolainen, J.; Herek, J. L.; Vanmaekelbergh, D.; Ruhman, S.; Mocatta, D.; Oron, D.; Aharoni, A.; Banin, U.; Bonn, M. *J. Phys. Chem. C* **2007**, *111*, 4146.
(145) Schaller, R. D.; Pietryga, J. M.; Klimov, V. I. *Nano Lett.* **2007**, *7*, 3469.
(146) Beard, M. C.; Knutsen, K. P.; Yu, P.; Luther, J. M.; Song, Q.; Metzger, W. K.; Ellingson, R. J.; Nozik, A. J. *Nano Lett.* **2007**, *7*, 2506.
(147) Kobayashi, Y.; Udagawa, T.; Tamai, N. *Chem. Lett.* **2009**, *38*, 830.
(148) Nair, G.; Bawendi, M. G. *Phys. Rev. B* **2007**, *76*, 081304.
(149) Pijpers, J. J. H.; Hendry, E.; Milder, M. T. W.; Fanciulli, R.; Savolainen, J.; Herek, J. L.; Vanmaekelbergh, D.; Ruhman, S.; Mocatta, D.; Oron, D.; Aharoni, A.; Banin, U.; Bonn, M. *J. Phys. Chem. C* **2008**, *112*, 4783.
(150) Ben-Lulu, M.; Mocatta, D.; Bonn, M.; Banin, U.; Ruhman, S. *Nano Lett.* **2008**, *8*, 1207.
(151) Nair, G.; Geyer, S. M.; Chang, L. Y.; Bawendi, M. G. *Phys. Rev. B* **2008**, *78*, 125325.
(152) Beard, M. C.; Midgett, A. G.; Law, M.; Semonin, O. E.; Ellingson, R. J.; Nozik, A. J. *Nano Lett.* **2009**, *9*, 836.
(153) McGuire, J. A.; Joo, J.; Pietryga, J. M.; Schaller, R. D.; Klimov, V. I. *Acc. Chem. Res.* **2008**, *41*, 1810.
(154) Midgett, A. G.; Hillhouse, H. W.; Hughes, B. K.; Nozik, A. J.; Beard, M. C. *J. Phys. Chem. C* **2010**, *114*, 17486.
(155) Mangolini, L.; Thimsen, E.; Kortshagen, U. *Nano Lett.* **2005**, *5*, 655.
(156) Jurbergs, D.; Rogojina, E.; Mangolini, L.; Kortshagen, U. *Appl. Phys. Lett.* **2006**, *88*, 233116.
(157) Murray, C. B.; Kagan, C. R.; Bawendi, M. G. *Science* **1995**, *270*, 1335.
(158) Gaponenko, S. V. *Optical Properties of Semiconductor Nanocrystals*; Cambridge University Press: Cambridge, UK, 1998.
(159) Mićić, O. I.; Jones, K. M.; Cahill, A.; Nozik, A. J. *J. Phys. Chem. B* **1998**, *102*, 9791.
(160) Collier, C. P.; Vossmeyer, T.; Heath, J. R. *Annu. Rev. Phys. Chem.* **1998**, *49*, 371.
(161) Leatherdale, C. A.; Kagan, C. R.; Morgan, N. Y.; Empedocles, S. A.; Kastner, M. A.; Bawendi, M. G. *Phys. Rev. B* **2000**, *62*, 2669.
(162) Porter, V. J.; Geyer, S.; Halpert, J. E.; Kastner, M. A.; Bawendi, M. G. *J. Phys. Chem. C* **2008**, *112*, 2308.
(163) Mentzel, T. S.; Porter, V. J.; Geyer, S.; MacLean, K.; Bawendi, M. G.; Kastner, M. A. *Phys. Rev. B* **2008**, *77*, 75316.
(164) Mićić, O. I.; Ahrenkiel, S. P.; Nozik, A. J. *Appl. Phys. Lett.* **2001**, *78*, 4022.
(165) Luther, J. M.; Beard, M. C.; Song, Q.; Law, M.; Ellingson, R. J.; Nozik, A. J. *Nano Lett.* **2007**, *7*, 1779.
(166) Talapin, D. V.; Murray, C. B. *Science* **2005**, *310*, 86.
(167) Wehrenberg, B. L.; Yu, D.; Ma, J. S.; Guyot-Sionnest, P. *J. Phys. Chem. B* **2005**, *109*, 20192.
(168) Murphy, J. E.; Beard, M. C.; Nozik, A. J. *J. Phys. Chem. B* **2006**, *110*, 25455.
(169) Law, M.; Luther, J. M.; Song, O.; Hughes, B. K.; Perkins, C. L.; Nozik, A. J. *J. Am. Chem. Soc.* **2008**, *130*, 5974.
(170) Liu, Y.; Gibbs, M.; Puthussery, J.; Gaik, S.; Ihly, R.; Hillhouse, H. W.; Law, M. *Nano Lett.* **2010**, *10*, 1960.
(171) Choi, J. J.; Luria, J.; Hyun, B. R.; Bartnik, A. C.; Sun, L. F.; Lim, Y. F.; Marohn, J. A.; Wise, F. W.; Hanrath, T. *Nano Lett.* **2010**, *10*, 1805.
(172) Zarghami, M. H.; Liu, Y.; Gibbs, M.; Gebremichael, E.; Webster, C.; Law, M. *ACS Nano* **2010**, *4*, 2475.
(173) Smith, B. B.; Nozik, A. J. *Nano Lett.* **2001**, *1*, 36.
(174) Nozik, A. J.; Memming, R. *J. Phys. Chem.* **1996**, *100*, 13061.
(175) Yu, D.; Wang, C. J.; Wehrenberg, B. L.; Guyot-Sionnest, P. *Phys. Rev. Lett.* **2004**, *92*, 4.
(176) Houtepen, A. J.; Kockmann, D.; Vanmaekelbergh, D. *Nano Lett.* **2008**, *8*, 3516–3520.
(177) Kraus, R. M.; Lagoudakis, P. G.; Muller, J.; Rogach, A. L.; Lupton, J. M.; Feldmann, J.; Talapin, D. V.; Weller, H. *J. Phys. Chem. B* **2005**, *109*, 18214.
(178) Wehrenberg, B. L.; Guyot-Sionnest, P. *J. Am. Chem. Soc.* **2003**, *125*, 7806.
(179) Yu, D.; Wang, C. J.; Guyot-Sionnest, P. *Science* **2003**, *300*, 1277.
(180) Urban, J. J.; Talapin, D. V.; Shevchenko, E. V.; Murray, C. B. *J. Am. Chem. Soc.* **2006**, *128*, 3248.
(181) Schaller, R. D.; Sykora, M.; Pietryga, J. M.; Klimov, V. I. *Nano Lett.* **2006**, *6*, 424.
(182) Shockley, W.; Queisser, H. J. *J. Appl. Phys.* **1961**, *32*, 510.

(183) Ross, R. T. *J. Chem. Phys.* **1966**, *45*, 1.
(184) Ross, R. T. *J. Chem. Phys.* **1967**, *46*, 4590.
(185) Green, M. A. *Solar Cells*; Prentice-Hall: Englewood Cliffs, NJ, 1982.
(186) Landsberg, P. T.; Nussbaumer, H.; Willeke, G. *J. Appl. Phys.* **1993**, *74*, 1451.
(187) Luque, A.; Martí, A. *Phys. Rev. Lett.* **1997**, *78*, 5014.
(188) Nozik, A. J. *Philos. Trans. R. Soc. London, Ser. A* **1980**, *A295*, 453.
(189) Pelouch, W. S.; Ellingson, R. J.; Powers, P. E.; Tang, C. L.; Szmyd, D. M.; Nozik, A. J. *Semicond. Sci. Technol.* **1992**, *7*, B337.
(190) Blackburn, J. L.; Ellingson, R. J.; Mićić, O. I.; Nozik, A. J. *J. Phys. Chem. B* **2003**, *107*, 102.
(191) Ellingson, R. J.; Blackburn, J. L.; Nedeljković, J. M.; Rumbles, G.; Jones, M.; Fu, H.; Nozik, A. *J.Phys. Rev. B* **2003**, *67*, 075308/1.
(192) Nakata, Y.; Sugiyama, Y.; Sugawara, M. In *Semiconductors and Semimetals*; Sugawara, M., Ed.; Academic Press: San Diego, 1999; Vol. 60.
(193) Hagfeldt, A.; Grätzel, M. *Acc. Chem. Res.* **2000**, *33*, 269.
(194) Moser, J.; Bonnote, P.; Grätzel, M. *Coord. Chem. Rev.* **1998**, *171*, 245.
(195) Grätzel, M. *Prog. Photovoltaics* **2000**, *8*, 171.
(196) Zaban, A.; Mićić, O. I.; Gregg, B. A.; Nozik, A. J. *Langmuir* **1998**, *14*, 3153.
(197) Vogel, R.; Hoyer, P.; Weller, H. *J. Phys. Chem.* **1994**, *98*, 3183.
(198) Weller, H. *Ber. Bunsenges. Phys. Chem.* **1991**, *95*, 1361.
(199) Liu, D.; Kamat, P. V. *J. Phys. Chem.* **1993**, *97*, 10769.
(200) Hoyer, P.; Könenkamp, R. *Appl. Phys. Lett.* **1995**, *66*, 349.
(201) Sambur, J. B.; Novet, T.; Parkinson, B. A. *Science* **2010**, submitted for publication.
(202) Greenham, N. C.; Peng, X.; Alivisatos, A. P. *Phys. Rev. B* **1996**, *54*, 17628.
(203) Greenham, N. C.; Peng, X.; Alivisatos, A. P. In *Future Generation Photovoltaic Technologies: First NREL Conference*; McConnell, R., Ed.; American Institute of Physics: Melville, NY, 1997.
(204) Huynh, W. U.; Peng, X.; Alivisatos, P. *Adv. Mater.* **1999**, *11*, 923.
(205) Dayal, S.; Kopidakis, N.; Olson, D. C.; Ginley, D. S.; Rumbles, G. *Nano Lett.* **2010**, *10*, 239.
(206) Arango, A. C.; Carter, S. A.; Brock, P. J. *Appl. Phys. Lett.* **1999**, *74*, 1698.
(207) Nozik, A. J.; Rumbles, G.; Selmarten, D. C. 2000, unpublished manuscript.
(208) Dabbousi, B. O.; Bawendi, M. G.; Onitsuka, O.; Rubner, M. F. *Appl. Phys. Lett.* **1995**, *66*, 1316.
(209) Colvin, V.; Schlamp, M.; Alivisatos, A. P. *Nature* **1994**, *370*, 354.
(210) Schlamp, M. C.; Peng, X.; Alivisatos, A. P. *J. Appl. Phys.* **1997**, *82*, 5837.
(211) Mattoussi, H.; Radzilowski, L. H.; Dabbousi, B. O.; Fogg, D. E.; Schrock, R. R.; Thomas, E. L.; Rubner, M. F.; Bawendi, M. G. *J. Appl. Phys.* **1999**, *86*, 4390.
(212) Mattoussi, H.; Radzilowski, L. H.; Dabbousi, B. O.; Thomas, E. L.; Bawendi, M. G.; Rubner, M. F. *J. Appl. Phys.* **1998**, *83*, 7965.
(213) Jiang, X. M.; Schaller, R. D.; Lee, S. B.; Pietryga, J. M.; Klimov, V. I.; Zakhidov, A. A. *J. Mater. Res.* **2007**, *22*, 2204.
(214) Cui, D.; Xu, J.; Zhu, T.; Paradee, G.; Ashok, S.; Gerhold, M. *Appl. Phys. Lett.* **2006**, *88*, 183111/1.
(215) Fritz, K. P.; Guenes, S.; Luther, J.; Kumar, S.; Saricifitci, N. S.; Scholes, G. D. *J. Photochem. Photobiol., A* **2008**, *195*, 39.
(216) McDonald, S. A.; Konstantatos, G.; Zhang, S. G.; Cyr, P. W.; Klem, E. J. D.; Levina, L.; Sargent, E. H. *Nature Mater.* **2005**, *4*, 138.
(217) Qi, L.; Cölfen, H.; Antonietti, M. *Nano Lett.* **2005**, *1*, 61.
(218) Watt, A. A. R.; Blake, D.; Warner, J. H.; Thomsen, E. A.; Tavenner, E. L.; Rubinsztein-Dunlop, H.; Meredith, P. *J. Phys. D: Appl. Phys.* **2005**, *38*, 2006.
(219) Luther, J. M.; Law, M.; Beard, M. C.; Song, Q.; Reese, M. O.; Ellingson, R. J.; Nozik, A. J. *Nano Lett.* **2008**, *8*, 3488.
(220) Clifford, J. P.; Johnston, K. W.; Levina, L.; Sargent, E. H. *Appl. Phys. Lett.* **2007**, *91*, 253117.
(221) Schoolar, R. B.; Jensen, J. D.; Black, G. M. *Appl. Phys. Lett.* **1977**, *31*, 620.
(222) Leschkies, K. S.; Beatty, T. J.; Kang, M. S.; Norris, D. J.; Aydil, E. S. *ACS Nano* **2009**, *3*, 3638–3648.
(223) Choi, J. J.; Lim, Y. F.; Santiago-Berrios, M. B.; Oh, M.; Hyun, B. R.; Sung, L. F.; Bartnik, A. C.; Goedhart, A.; Malliaras, G. G.; Abruna, H. D.; Wise, F. W.; Hanrath, T. *Nano Lett.* **2009**, *9*, 3749.
(224) Luther, J.; Gao, J.; Lloyd, M. T.; Semoni, O. E.; Beard, M. C.; Nozik, A. J. *Adv. Mater.* **2010**, *22*, 3704.

CR900289F